

FUNCTIONALIZATION OF GOLD AND GLASS SURFACES WITH MAGNETIC
NANOPARTICLES USING BIOMOLECULAR INTERACTIONS

A Thesis

Submitted to the Graduate Faculty of the
Louisiana State University and
Agricultural and Mechanical College
In partial fulfillment of the
requirements for the degree of
Master of Science in
Biological and Agricultural Engineering

in

The Department of Biological and Agricultural Engineering

by
Bala Sesha Giri Rao Nidumolu
B.S., Jawaharlal Nehru Technological University, 2001
May 2005

Acknowledgments

I would like to express my deepest and sincere gratitude to Dr. W. Todd Monroe for his guidance and support through this entire graduate program as my major professor. I would also like to thank the members of my graduate committee, Dr. Challa Kumar, Dr. Daniel Thomas and Dr. Cristina M. Sabliov, for their advice and assistance. I would like to also thank Cindy Henk, Dr. Orhan Kizilkaya, and Dr. Jiechao Jiang for access to their equipment, without which this research would not be possible. Also, I would like to thank Michelle C. Urbina for her help in synthesis and functionalization of nanoparticles.

My earnest appreciation to Dr. Daniel Thomas and the Department of Biological and Agricultural Engineering for the support and graduate assistantship, which has supported me through this time of study. I would like to acknowledge my fellow graduate students: Rick Blidner, Brendan McAdams, Bilal Ghosn, and Julianne Forman, for all their support and time that allowed for this to happen. Finally, I would like to thank my family for all their encouragement and understanding throughout this entire process. I would like to thank Rick Blidner and Julianne Forman for their valuable feedback on my thesis.

Table of Contents

| | |
|---|------|
| Acknowledgments..... | ii |
| List of Tables..... | v |
| List of Figures..... | vi |
| Abstract..... | viii |
| Chapter 1: Introduction..... | 1 |
| 1.1 Iron Oxide Magnetic Nanoparticle System..... | 7 |
| 1.1.1 Relative Magnetic Principles..... | 7 |
| 1.1.2 Magnetic Properties of Small Particles..... | 9 |
| 1.1.3 Classification of Magnetic Nanoparticles..... | 10 |
| 1.1.4 Iron Oxides..... | 11 |
| 1.1.5 Advantages of Nanoparticles over Microparticles in the Detection System..... | 12 |
| 1.1.6 Applications of Nanoparticles..... | 14 |
| 1.1.7 Applications of Magnetic Nanoparticles | 15 |
| 1.2 Self-Assembled Monolayers..... | 18 |
| 1.2.1 Background..... | 18 |
| 1.2.2 Preparation of SAMs..... | 20 |
| 1.2.3 Characterization of Monolayers..... | 20 |
| 1.2.4 Applications of Self-Assembled Monolayers..... | 22 |
| 1.2.5 Biotin-SAM's..... | 24 |
| 1.3 Characterization Techniques | 26 |
| 1.3.1 Transmission Electron Microscopy (TEM) and Scanning Electron Microscopy (SEM)..... | 26 |
| 1.3.2 Energy Dispersive X-ray Spectrometry (EDS)..... | 27 |
| 1.3.3 Fourier Transform Infrared Spectroscopy (FT-IR)..... | 27 |
| 1.3.4 Reflection Absorption Infrared Spectroscopy (RAIRS)..... | 28 |
| 1.3.5 Fluorescent Microscopy..... | 29 |
| 1.3.6 X-ray Photoelectron Spectroscopy (XPS)..... | 29 |
| Chapter 2: Functionalization and Characterization of Gold and Glass Surfaces..... | 31 |
| 2.1 Introduction..... | 31 |
| 2.2 Material and Methods..... | 34 |
| 2.2.1 Synthesis of Nanoparticles | 34 |
| 2.2.2 Functionalization of Nanoparticles with Streptavidin | 35 |
| 2.2.3 Immobilization of Biotin-HPDP on Gold | 35 |
| 2.2.4 Binding of Streptavidin to Biotinylated Gold Surfaces..... | 36 |
| 2.2.5 Binding of Streptavidin Conjugated Nanoparticles to Biotinylated gold Surface..... | 37 |
| 2.2.6 Binding of Sulpho NHS-biotin to Aminated slide..... | 37 |

| | |
|---|----|
| 2.2.7 Binding of Streptavidin Conjugated Nanoparticles to Biotinylated Glass Slide..... | 38 |
| 2.3 Characterization of Functionalized Gold surfaces..... | 38 |
| 2.3.1 Transmission Electron Microscopy (TEM)..... | 38 |
| 2.3.2 Fourier Transform Infrared Spectroscopy (FT-IR)..... | 38 |
| 2.3.3 Fluorescent Microscopy..... | 39 |
| 2.3.4 X-ray photoelectron Spectroscopy (XPS)..... | 39 |
| 2.3.5 Scanning Electron Microscopy (SEM)..... | 40 |
| 2.4 Results and Discussion..... | 40 |
| Chapter 3: Conclusions and Future Considerations | 49 |
| 3.1 Conclusions | 49 |
| 3.1 Future Considerations | 51 |
| References..... | 54 |
| Vita..... | 64 |

List of Tables

| | |
|--|----|
| 1.1 Estimated Maximum Single-Domain Size for Spherical Particles..... | 9 |
| 1.2 Magnetization Values for Metals and Metal oxides..... | 10 |
| 1.3 Chemical Composition and Magnetic Properties of Different Iron Oxides..... | 11 |
| 1.4 Physical Properties of Magnetite and Maghemite..... | 11 |

List of Figures

| | |
|---|----|
| 1. Mechanism of Separation of Substances using Nanoparticles..... | 2 |
| 2. Schematic Diagram of the BARC Sensor | 4 |
| 3. Comparison of Magnetization per unit mass of Nano and Microparticles... | 12 |
| 4. Magnetization Curves of (a) Nano and (b) Microparticles..... | 13 |
| 5. Different Attachment Groups and Substrates for the Formation of SAMs... | 19 |
| 6. IR Absorbance for Common Functional Groups..... | 28 |
| 7. Schematic of Nanoparticle Based Biosenor..... | 33 |
| 8. Reduction of the Biotin-HPDP disulphide bond using Tri-n-butylphosphine..... | 36 |
| 9. Immobilization of Sulpho NHS-biotin on Aminated Glass Slide..... | 37 |
| 10. Transmission Electron Micrograph of Iron Oxide Nanoparticles..... | 40 |
| 11. FT-IR of Unfunctionalized and Functionalized Nanoparticles..... | 41 |
| 12. FT-IR of Biotin-HPDP Immobilized on Gold..... | 42 |
| 13. FT-IR of Deposited and Captured Nanoparticles on Gold Surface..... | 43 |
| 14. Phase and Fluorescent Microscopy Images of Streptavidin-Conjugated Nanoparticles Captured by Biotinylated Gold SAMs..... | 43 |
| 15. Phase and Fluorescent Images of Streptavidin Conjugated Nanoparticles Deposited on Gold vs Glass Surfaces Illustrate Detection Limits of the Fluorescent Technique..... | 44 |
| 16. Photo-Bleaching of FITC-Streptavidin Wet vs Dry Droplets on Gold..... | 44 |
| 17. Phase and Fluorescent Images of Nanoparticles Captured on Aminated Glass Slide..... | 45 |
| 18. XPS of Gold Surface (a) Before and (b) After the Functionalization with Biotin-HPDP..... | 46 |
| 19. SEM Image of Biotinylated Gold Surface with Aggregated Streptavidin Conjugated Iron Nanoparticles for Elemental EDS Analysis..... | 46 |

| | |
|---|----|
| 20. EDS Analysis of Biotinylated Gold Surface with Streptavidin Conjugated (A) Small and (B) Large Nanoparticles..... | 47 |
| 21. SEM Images of Functionalized Nanoparticles Immobilized on Aminated Glass Surface..... | 47 |

Abstract

Advances in nanotechnology have enabled the production and characterization of magnetic particles with nanometer-sized features that can be functionalized with biological recognition elements for clinical and biosensing applications. In the present study the synthesis and interactions between self assembled monolayers (SAMs) and functionalized nanoparticles have been characterized. Size and shape of magnetic nanoparticles synthesized wet chemically starting from ferrous and ferric salts were verified by transmission electron microscopy (TEM). These nanoparticles were then conjugated with FITC-labeled streptavidin through carbodiimide (EDC) chemistry. SAMs of thiol-capped biotins were synthesized on gold surfaces for capture of the conjugated nanoparticles. Characterization of nanoparticle functionalization and binding was performed using fluorescent microscopy, Fourier transform infrared spectroscopy (FT-IR), X-ray photoelectron spectroscopy (XPS), transmission electron microscopy (TEM) and scanning electron microscopy (SEM) with energy dispersive spectrometry (EDS). FT-IR spectra confirm the binding of biotin on gold via sulphur linkages. Fluorescent microscopy and XPS show streptavidin bound to the biotinylated gold surfaces. Elemental characterization from EDS indicates the binding of streptavidin-conjugated nanoparticles to biotinylated gold surfaces. Together, these techniques have application in studying the modification and behavior of functionalized nanoparticles for biological and other applications.

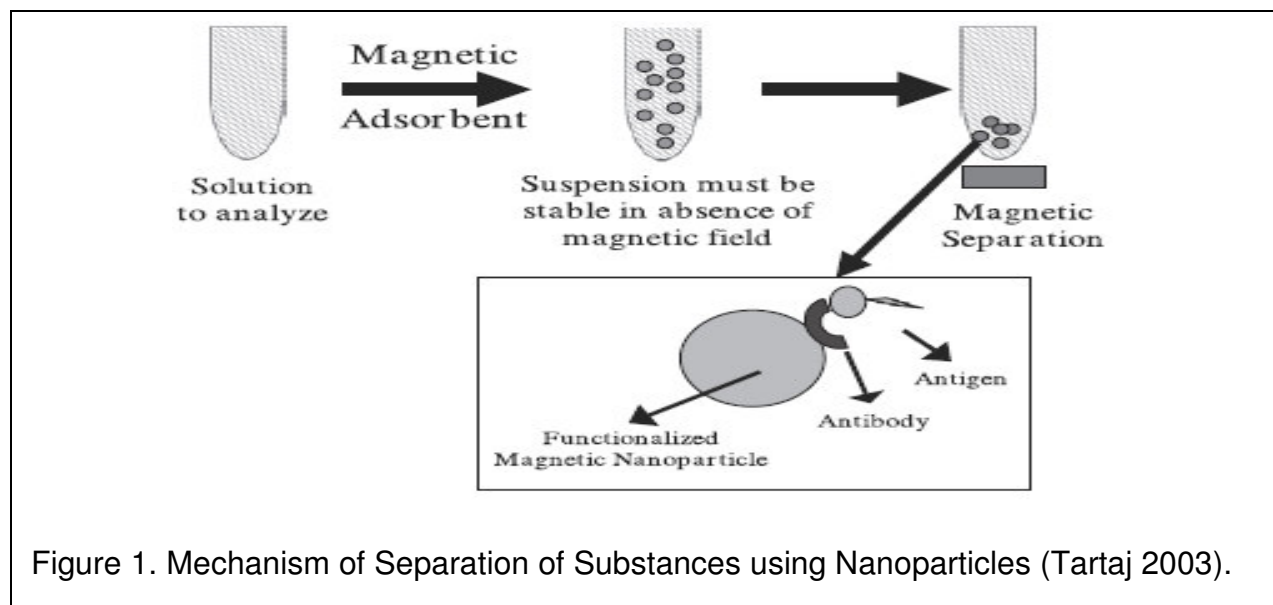
Chapter 1

Introduction

The study of nanometer-sized objects has generated considerable interest with respect to both scientific and commercial applications, such as measuring low concentrations of bacteria, magnetic resonance imaging (Artemov 2003), more efficient site-specific drug delivery (Forbes 2003; Lubbe 2001), detection of proteins (Cao 2003), and separation and purification of biological molecules and cells (Molday 1982). Various types of nanoparticles are being used in biosensing schemes to show improvements over microparticles. Gold nanoparticles used in the fabrication of a glucose sensor based on aggregation and dissociation of 20nm gold particles show changes in plasmon absorption induced by the presence of glucose (Aslan, 2004). Concanavalin A has been used to aggregate gold nanoparticles coated with high-molecular weight dextran, which shifts and broadens the gold plasmon absorption. After the addition of glucose, a reduction in plasmon absorption occurs, this is detected by the sensor. Functionalization of magnetic beads with biological recognition elements that can bind to specific targets has several advantages in the detection of biomolecules compared to radioactive, electrochemical, and optical methods (Rife 2003). For example, radioimmunoassay requires expensive instrumentation and handling of potentially hazardous radioactive materials; whereas, magnetic bead detection is cheap, efficient, and safe.

Magnetic nanoparticles have an additional advantage of being easily manipulated by permanent magnets or electromagnets, independent of normal microfluidic or biological processes. The separation of biomolecules for purification or characterization

is another application of magnetic particles (Pankhurst 2003). Magnetic separation is a well-established alternative to centrifugal separation of complex chemical or biological solutions. Typically iron oxide particles are first encased in a biocompatible coating to form small beads. The beads are then functionalized with a biological or chemical agent known to bind to a specific target. Upon placing the beads in solution, any target cells or molecules can be captured by the functionalized surfaces. A permanent magnet placed at the side of the solution container induces a magnetic moment in each of the freely floating beads and sets up a field gradient across the solution. The magnetized beads will move along the field lines and aggregate together towards the magnet, separating their bound targets from the bulk solution (Figure 1).



Nanoparticles have several advantages in detecting biological molecules compared to microparticles, such as high magnetization per unit weight, ability to remain in suspension for longer periods of time without aggregating, and faster velocities in solution (Moller 2003). Biomedical applications using nanoparticles require narrow size distribution and compatibility with surface modifiers i.e. nonimmunogenic,

nonantigenic and resistant to protein adsorption (Pankhurst 2003). Here we demonstrate the synthesis and functionalization of nanoparticles that could be utilized in any of these aforementioned applications.

The recognition and capture of molecules at solid surfaces has numerous bioanalytical applications in bio- and immunosensor diagnostic devices (Yam 2002). The immobilization of bio-recognition molecules, such as nucleic acids, and ligands on solid surfaces plays an important role in the development of such devices. For efficient immobilization, the maximum biochemical activity and minimum nonspecific interactions must be achieved. Using a system that couples proteins with nanoparticles, the efficiency of the immobilization can be increased. Here we demonstrate a system for functionalization of magnetic nanoparticles in addition to functionalized surfaces for their binding in an effort to move towards nanoparticle based bio-recognition schemes.

The biotin and streptavidin couple is an ideal model for these types of bioconjugation applications because of its high binding affinity ($K_a=10^{15} \text{ M}^{-1}$) and high specificity (Yam 2002). Each streptavidin has four binding sites for biotin positioned in pairs on opposite domains of the protein molecule. Nanoparticle-protein binding occurs between the amine residues on the nanoparticle surface and the carbodiimide-activated carboxylic group of streptavidin (Kumar 2004). Several forms of thiolated biotin are now commercially available that can be immobilized to gold surfaces via sulphur linkages (Pradier 2002). The high affinity of gold for sulphur-containing molecules generates well-ordered monolayers termed self-assembled monolayers (SAMs). In this ongoing effort we describe the synthesis of streptavidin-functionalized magnetic nanoparticles

and characterize their binding to biotinylated SAMs on gold for biological recognition applications.

A model system using functionalized magnetic particles and surfaces for biosensing was developed by Edelstein's group, the Bead ARray Counter (BARC), which is based on the capture and detection of paramagnetic micro-beads (0.7 μm) on a chip containing an array of giant magnetoresistive (GMR) sensors. A non magnetic conducting layer is used to separate magnetic thin films which can be aligned by an external magnetic field that changes the resistance of the device (Edelstein 2000). The local magnetic fields can be measured by measuring the change in the resistance detected by GMR. Iron oxide superparamagnetic particles coated with a polymer onto which proteins or antibodies are attached are used to detect bacteria.

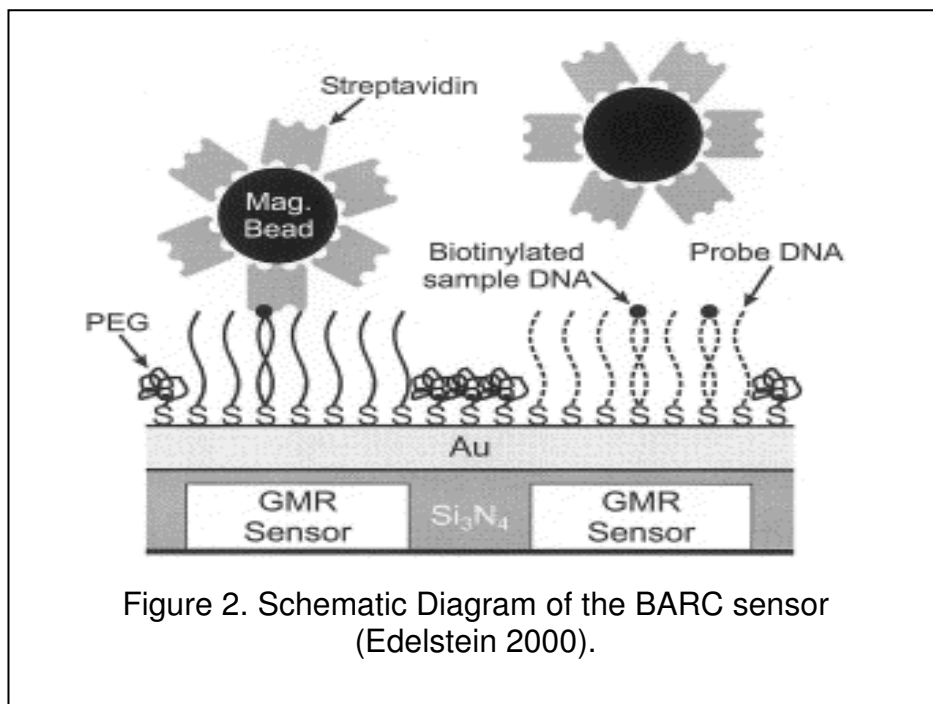


Figure 2. Schematic Diagram of the BARC sensor (Edelstein 2000).

The BARC biosensor system is illustrated in Figure 2. Micro-contact pen spotting was used to immobilize thiolated DNA probes, complementary to the DNA to be

detected, onto a gold layer on the solid substrate chip directly above the GMR sensors. The biotinylated DNA from a PCR reaction is injected into the instrument. If the complementary probe is present on the GMR chip, the PCR products will hybridize. The solution of streptavidin-coated beads is then added to the chip fluidics. The beads will specifically bind to the biotinylated sample DNA hybridized to the chip surface. The non-specifically bound beads to the GMR surface can be removed by applying a magnetic field gradient with the electromagnet. When an AC magnetic field is applied, the beads will be magnetized which generates sensing fields. The number of beads will be detected by GMR sensor, the intensity and location of the signal will indicate the concentration and identity of pathogens present in the sample. O-(2-mercaptoethyl)-o'-methyl-polyethylene glycol 5000 (PEG) has been used to prevent non-specific adhesion of sample DNA and the magnetic beads on the GMR surface. Similarly in our study pyridine 2-thiol has been used as a spacer to prevent non-specific adhesion of magnetic nanoparticles onto the gold surface (Zimmermann 1994).

A similar magnetic detection system, which is based on nanoparticles (200nm) and self-assembled monolayers with biotin-streptavidin coupling, has been recently developed by Arakaki's group (Arakaki 2004). Octadecyltrimethoxysilane (ODMS) self-assembled monolayers were formed on a silicon oxide surface which was patterned by irradiation with oxygen plasma. In this system, ODMS was used as a spacer to avoid nonspecific adsorption of nanoparticles on the silicon oxide surface whereas in our technique an internal spacer, to the biotin-HPDP pyridine 2-thiol was used to functionalize the gold surface and no spacer was used to functionalize glass surface with sulpho-NHS biotin. 3-aminopropyltriethoxysilane (APS) was selectively immobilized

in certain locations and then linked to sulpho-NHS-LC-LC-biotin using NHS EDC chemistry. A sandwich method of indirect coupling of nanoparticles to streptavidin was employed. The amine groups of purchased magnetite nanoparticles were reacted with sulpho-NHS-LC-LC-biotin and then functionalized with streptavidin. Linked layers of nanoparticle-biotin-streptavidin-biotin-SAM were characterized by optical microscope, magnetic force microscope (MFM), scanning electron microscope (SEM). Sodium dodecylsulphate (SDS) was used as a surfactant to minimize the aggregation of particles. This study is based on similar techniques except that the self assembled monolayers of biotin-HPDP and sulpho NHS biotin were formed on gold or aminated glass substrates directly. Direct functionalization of synthesized nanoparticles with streptavidin is done by using EDC chemistry. No surfactant was used to avoid aggregation of particles. Fourier transform infrared spectroscopy (FT-IR), fluorescent microscopy, Scanning electron microscopy (SEM), Transmission electron microscopy (TEM), and X-ray photoelectron microscopy (XPS) were used to characterize the surfaces.

Nanoparticles are also used in the fabrication of CMOS Hall effect sensors which are useful in the detection of specific targets (Turgut Aytur 2002; Besse 2002; Li 2002). Enzyme-Linked Immunosorbent Assay (ELISA), which is based on specific interactions between antibody and antigen, uses enzymes as labels in the detection. Precise quantitative analysis is difficult with the ELISA technique. There are many advantages of usage of magnetic particles as labels. First, there is very little native magnetic signal present in biological samples which will eliminate the background problem. Second, the particles can be manipulated by an external magnet. Third, they

are not affected by chemical and optical environment of the sensor. Fourth, there are many quantitative sensing devices such as GMR, piezo-resistive cantilevers, superconducting quantum interference device (SQUID), anisotropic magnetoresistive (AMR) rings etc. are commercially available.

One other type of biosensor utilizing nanoparticles, SQUID and antibody-antigen interactions to detect molecules, structures and microorganisms has been developed by Chemla and coworkers (Chemla 2000). The sensor consists of a microscope based on a high-transition temperature DC SQUID, a mylar film to which the targets have been bound which is placed 40 μ m from the SQUID. Superparamagnetic nanoparticles having antibodies are passed on the mylar film and simultaneously a magnetic field is applied. Due to the specific interactions between the antibody and target interactions a strong bond will occur and due to the presence of the magnetic field the nanoparticles develop a net magnetization. When the field is turned off the unbound particles relax rapidly which results in no measurable signal. The bounded particles relax slowly and produce a slowly decaying magnetic flux, which can be detected by the SQUID.

1.1 Iron Oxide Magnetic Nanoparticle System

1.1.1 Relevant Magnetic Principles

Magnetism is a force between electric currents: two parallel currents in the same direction attract, in opposite directions repel. Most material possesses magnetic properties which are negligibly small to measure. The magnetic properties of matter are governed by electrons. In some materials magnetic properties depends on the spin of the electrons. The spin can be oriented either up or down in direction (Beiser 1973). The second is similar to a current loop where electrons circulated around the nucleus of the

atom (Beiser, 1973). These charges produce magnetic lines of force known as the dipole (Kittel 1976). The strength of the dipole is measured with the magnetic moment of the material. The magnetic moment of the electron is due to its spin around the orbit. Magnetic field strength (H) is the amount of magnetizing force. It is proportional to the length of a conductor and the amount of electrical current passing through the conductor (Sorensen 2001). Magnetic induction (B) is the EMF induced into a conductor when it cuts the magnetic lines of force.

Magnetization (M) is the density of net magnetic dipole moments (μ) in a material.

$$M = \mu_{\text{total}} / V \text{ ampere/meter} \quad (\text{Equation 1})$$

The magnetic induction (B) of a material is a function of magnetic field strength (H) and the magnetization (M).

$$B = \mu_0 (M + H) \text{ Teslas} \quad (\text{Equation 2})$$

μ_0 is the permeability of vacuum.

Magnetic susceptibility is a measure of the ease with which particular materials are magnetized in the presence of an external magnetic field

$$K = M/H \quad (\text{Equation 3})$$

Materials are classified into five types by their response to an external applied magnetic field. Ferromagnetic materials are materials which can be permanently magnetized upon application of an external magnetic field. This external field is typically applied by another permanent magnet, or by an electromagnet. Unequal magnetic moment of the atoms on different sublattices produces a spontaneous magnetization in a material. This happens when the sublattices consist of different materials or ions (such as Fe^{2+} and Fe^{3+}). These type materials are classified as ferrimagnetic materials. Antiferromagnetic

materials possess atomic moments of equal magnitude arranged in an antiparallel fashion (Li 1997). The coupling of atomic magnets can be disrupted by heating and disappears entirely above a certain temperature, called the Neel temperature above which they exhibit paramagnetic behavior. Materials in which the cancellation of magnetic moments of electrons is incomplete are treated as paramagnetic materials. Hence, they possess a small positive magnetic susceptibility ($\chi \approx 0$) (Burts 2000). In diamagnetic materials the magnetic fields produced by the orbital motion of electrons aligns opposite to the external magnetic field. They have negative susceptibility ($\chi < 0$) and weakly repel an applied magnetic field (Li 2000).

1.1.2 Magnetic Properties of Small Particles

The domain wall width of a magnetic material is a function of the size, type of the lattice and the exchange energy. Usually the wall is approximately a few hundred angstroms thick (Li 1997; Smit 1959). The existence of the domain wall is energetically unfavorable when the particle size crosses a certain limit (Ozaki 2000).

Table 1.1. Estimated Maximum Single-domain Size for Spherical particles (Lesliepelecky 1996; Kittel 1946; Sorensen 2001).

| Material | Ds (nm) |
|--------------------------------|---------|
| Fe | 14 |
| Co | 14 |
| Ni | 55 |
| $\gamma\text{-Fe}_2\text{O}_3$ | 166 |
| Fe_3O_4 | 128 |

Table 1.1 shows the critical size range of different nanoparticles to have single domain walls. Nanoparticles have high magnetic moment compared to the transition metal ions of respective materials; hence saturation magnetization can be reached

at very low magnetic fields (Blum 1997). Coercive force is the value of magnetizing force required to reduce the flux density to zero. Single domain particles possess a large coercive force due to the magnetocrystalline and shape anisotropies for nonspherical particles.

1.1.3 Classification of Magnetic Nanoparticles

Metals such as Nickel (Ni), Cobalt (Co), Fe, Fe₃O₄ and γ -Fe₂O₃ and their oxides are used to synthesize magnetic particles capable of forming superparamagnetic dispersion in a carrier fluid of length scales from 1 to 100nm. The pure metals have the highest magnetic susceptibility summarized in Table 1.2.

Table 1.2. Magnetization Values for Metals and Metal oxides (Sorensen 2001).

| Substance | Saturation Magnetization (M _s) (emu/ cm ⁻³) at 298K |
|--|---|
| Ni | 485 |
| Co (cubic) | 1400-1422 |
| Fe (cubic) | 1700-1714 |
| γ -Fe ₂ O ₃ | 394 |
| FeO.Fe ₂ O ₃ | 480-500 |
| MnO.Fe ₂ O ₃ | 410 |
| CoO .Fe ₂ O ₃ | 400 |
| NiO.Fe ₂ O ₃ | 270 |
| CuO.Fe ₂ O ₃ | 135 |

When exposed to atmosphere Ni, Co and Fe oxidize to NiO, CoO and FeO alloys, which are antiferromagnetic in nature. These metals are also toxic in nature. Even though iron oxides have low initial magnetization, they are useful in oxygen rich environments because of their lower oxidation capacity. Because of these facts, iron oxides are most commonly used for particle synthesis.

1.1.4 Iron Oxides

The composition and magnetic properties of different iron oxides are shown in Table 1.3. Due to the ferrimagnetic nature of iron oxides such as $\gamma\text{-Fe}_2\text{O}_3$, Fe_3O_4 and $\text{MnO}\cdot\text{Fe}_2\text{O}_3$ these are more efficient in synthesizing nanoparticles. Ferromagnetic materials such as transition metals display a higher magnetic response than ferrimagnetic materials. However due to the low oxidizing nature of ferrimagnetic materials they maintain stable magnetic response.

Table 1.3 Chemical Composition and Magnetic Properties of Iron Oxides (Cornell 1991).

| Mineral | Formula | Magnetic response |
|---------------|---|----------------------|
| Goethite | $\alpha\text{-FeOOH}$ | antiferromagnetic |
| Akaganeite | $\beta\text{-FeOOH}$ | antiferromagnetic |
| Lepidocrocite | $\gamma\text{-FeOOH}$ | antiferromagnetic |
| Ferrihydrite | $\text{Fe}_5\text{HO}_8\cdot 4\text{H}_2\text{O}$ | antiferromagnetic |
| Hematite | $\text{A-Fe}_2\text{O}_3$ | Weakly ferromagnetic |
| Maghemite | $\Gamma\text{-Fe}_2\text{O}_3$ | ferrimagnetic |
| Magnetite | Fe_3O_4 | ferrimagnetic |

The physical properties of the most commonly used iron oxides are magnetite (Fe_3O_4) and maghemite ($\gamma\text{-Fe}_2\text{O}_3$) are summarized in table 1.4. From the table it is clear that both display ferrimagnetism, however the saturation magnetization of maghemite is lower than that of magnetite. Maghemite comprised solely of Fe^{3+} ions and magnetite is comprised of Fe^{2+} and Fe^{3+} in a 1:2 molar ratio.

Table 1.4 Physical Properties of Magnetite and Maghemite (Tebble 1996).

| | Crystal system | Cell dimensions (nm) | Density (g/cm ³) | Color | Magnetic susceptibility (emu/g) | Curie temperature (K) |
|-----------|---------------------|----------------------|------------------------------|---------------|---------------------------------|-----------------------|
| Magnetite | Cubic | $a_0=0.839$ | 5.26 | Black | 90-98 | 850 |
| Maghemite | Cubic or tetragonal | $a_0=0.834$ | 4.87 | Reddish-brown | 76-81 | 820-986 |

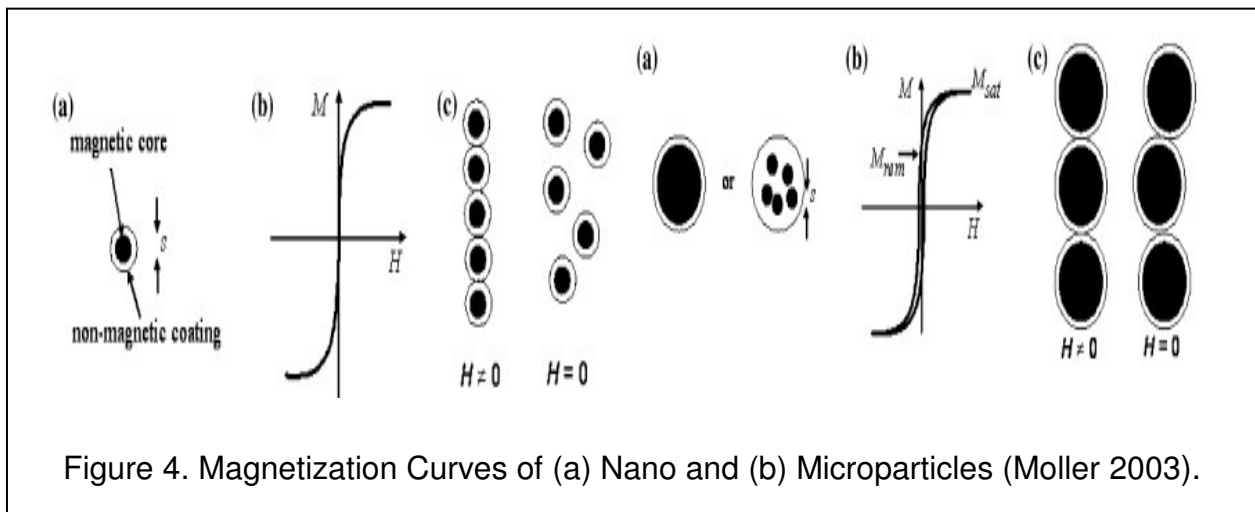
1.1.5 Advantages of Nanoparticles over Micro Particles in Detection system

| | |
|--|--|
| Mass of 10 nm dia magnetite nanoparticle | = $4 \pi /3 (5 \times 10^{-7})^3 \times \text{Density}$ = $4 \times 22 \times 125 \times 10^{-21} \times 5.189 / 21$ = $2.718 \times 10^{-18} \text{ g}$ |
| No of nanoparticles / g | = 3.67×10^{17} |
| Magnetization per particle | = $1.77 \times 10^{-16} \text{ emu}$ |
| Magnetization per gram weight of particles | = 65 emu |
| Mass of 3.0 μm dia microparticles beads | = $4\pi/3 (3 \times 10^{-4})^3 \times \text{Density}$ = $4 \times 22 \times 27 \times 10^{-12} \times 1.3$ = $147.085 \times 10^{-12} \text{ g}$ |
| No of Dyna beads / g | = 6.8×10^9 |
| Magnetization per particle | = $1.47 \times 10^{-9} \text{ emu}$ |
| Magnetization per gram weight of particles | = 10 emu |

Figure 3. Comparison of Magnetization per unit mass of Nano and Microparticles.

Figure 3 shows magnetization per unit weight of nano and microparticles. It also shows the number of particles present in 1mg of respective solutions. Because the size of nanoparticles is much smaller than microparticles, the number of particles present in a unit weight of the substance is greater for nanoparticles. One mg of 10nm nanoparticles has 3.67×10^{14} particles and hence can bind to a greater number of biomolecules than 1mg of 3 μm diameter microparticles having 6.8×10^6 particles. The magnetic moment of the nanoparticles is greater compared to microparticles. As there are more nanoparticles attached to a particular area compared to microparticles, the sensitivity is greater, because the number of attached streptavidin proteins will be greater. As the size of the particle is larger, the magnetic interaction between the particles is greater. Thus the magnetic moment of the nanoparticles is greater compared to micro particles and hence the sensitivity for detection is also greater. Another advantage of nanoparticles is the ability to remain in suspension after removal

of magnetic field. Figure 4 shows the comparison of magnetization properties of micro and nanoparticles (Moller 2003). When particles having diameters in the range of 5-100nm are used, the magnetization curve shows no hysteresis. This means that after removal of the field they have no remnant magnetization. This has special advantages of separating the nanoparticles from biomaterial of interest using a magnetic field without agglomeration. Microparticles have a multi-domain structure and are characterized by a hysteretic magnetization characteristic. Hence after removal of field, microparticles have a non-zero magnetization which leads to aggregation. Under the influence of magnetic field the microparticles acquire magnetization and coalesce into a supraparticle structure, which is a chain-like columnar structure in the direction of magnetic field. Due to mutual magnetization, the aggregate has a stronger remnant magnetic moment compared to the same number of single particles which will send false signals to the sensor (Moller 2003). Another advantage of nanoparticles based on their size is the lesser alteration of the biomolecule to which it is bound and the large surface-to-volume ratio for chemical binding.



1.1.6 Applications of Nanoparticles

In addition to the aforementioned cases, iron oxide nanoparticles have many applications ranging from catalysis to biosensing. For example, the synthesis of single-walled nanotubes with uniform diameter of 1.8nm and 3nm can be enhanced by nanoparticle catalysts. In this technique chemical vapor deposition is used to deposit nanoparticles on a flat surface prior to the carbon nanotube growth. Particles serve as nucleation sites where the tubes prefer to grow. Ago's group used cobalt nanoparticles as catalysts in the growth of multiwall carbon nanotubes (MWNTs) aligned perpendicular to a substrate (Ago 2000). Peng's group used iron nanoparticles as catalysts to grow single-walled carbon nanotubes aligned parallel to the substrate (Peng 2003). Zirconia nanoparticles have also been used to prevent the agglomeration of iron oxide nanoparticles (Han 2004). Gold nanoparticles are used in developing a nanobiosensor which is able to recognize and detect specific DNA sequences (Maxwell 2002). The advantage of this technique is that the nanoparticle probes do not require a stem like molecular beacons. Fluorescence detection can be done in single step (without washing or separation). Nanoparticles conjugated with biomolecules are used in the detection of antigens (Huhtinen 2004). Huhtinen's group used europium (III)-labeled nanoparticles coated with antibodies or streptavidin to detect prostate-specific antigen in serum. Nanoparticles are also useful in altering the properties of certain materials. For example, carbonitride nanoparticles can be used to increase the creep resistance of steel. Nanoparticles have several applications in printing industry as well (Giorgi 2002). Acidification of old manuscripts is a problem that must be addressed to prevent damage. Calcium hydroxide nanoparticles have been used to deacidify the

cellulose fibers. When these particles are deposited onto paper cellulose fibers, it deacidifies them, reacting with carbon dioxide from air and forming calcium carbonate on the paper fibers. With this process pH can be controlled for long durations. Layer-by-layer deposition of manganese-di-oxide (MnO_2) nanoparticles is used in the fabrication of a lactase biosensor (Xu 2005). The nanoparticles deposited at the gate surface acts as oxidants to react with H_2O_2 . When lactate is added, a change in pH occurs, which is detected by the sensor. Silver nanoparticles are used in fabrication of nitric oxide (NO) biosensor (Gan 2004). In this nanoparticles are used as catalysts in the reduction reaction between NO and hemoglobin (Hb).

1.1.7 Applications of Magnetic Nanoparticles

Magnetic nanoparticles also have several applications in the biomedical field. For example, hyperthermia is a process used to raise the temperature of a region of a body with local infection (Hilger, 2004). Infected cells can be killed by exposing them to local temperatures of 41 to 42°C. Iron-oxide nanoparticles are used for this application (Gilchrist 1957). External alternating magnetic fields can be used to heat a magnetic material which occurs during the reorientation of the magnetization of magnetic material having low electrical conductivity (Hiergeist 1999). The advantage of this technique over the other techniques such as multimodal cancer therapies is that it can be restricted to the particular diseased region. In this case nanoparticles are much more useful than microparticles because of the high penetration power into tissue at tolerable AC magnetic fields (Chan 1993; Rosensweig 2002). One other application of nanoparticles is in drug delivery (Forbes 2003; Lubbe 2001). In this technique the drug is attached to the magnetic nanoparticle and injected into the patient's bloodstream. They are

delivered to the specific site by using an external magnetic field. This occurs when magnetic forces exceed the blood flow rates to position nanoparticles at directed sites. The ability of magnetic nanoparticles to self-assemble has many applications. First, the surface on which self assembly occurs is a functionalized polymer coating. Particles having oleic acid/oleyl amine stabilizers are added to the polymer layer and the reaction occurs. In this reaction the particle stabilizers are replaced with a functional group of polymer by ligand exchange processes and a strong monolayer particle assembly is formed (Sun, 2002).

Self assembly of nanoparticles is used in the fabrication of ultrahigh-density data storage media (Weller 1999) and giant magneto-resistive properties films (Maekawa.S 1998). AFM probes can be functionalized with magnetic nanoparticles which can be used for high sensitive magnetic force sensing at high spatial resolution (Sqalli 2000). Nanoparticles are also used in increasing the activity of enzyme used for glucose sensing (Rossi 2004). In this technique enzyme glucose oxidase is covalently immobilized onto the magnetite nanoparticles using glutaraldehyde as cross-linking agent. This increases the number of active enzymatic sites compared to the process where enzyme is physically adsorbed onto the particle surface. Covalent immobilization also increases the thermal stability and the lifetime of enzyme molecules. Glucose oxidase-coated magnetite particles can be separated from analyte molecules by using magnetic fields, which has advantage of re-usage of particles for several processes. Bioactivity of enzyme molecules covalently attached to nanoparticles is greater compared to microparticles because of the high surface area of a given mass of nanoparticles. Zhang's group showed that by attaching magnetite nanoparticles to the

poly (ethylene glycol) (PEG), folic acid (FA), and their conjugate PEG-FA, the intracellular uptake of the nanoparticles to human breast cancer cells can be improved (Zhang 2005). Magnetite nanoparticles can be conjugated to PEG-FA using NHS EDC chemistry. The results showed that the PEG-FA coated nanoparticles exhibited higher efficiency compared to PEG or FA coated particles. Similarly magnetite nanoparticles are used to improve the activity, stability, and efficiency of the enzyme cholesterol oxidase (CHO), which has applications in biological and clinical fields.

Perez's group used magnetic nanoparticles in the fabrication of magnetic relaxation switches (MRS) (Perez 2002). Results showed that MRS nanoassemblies can act as biosensor to recognize and monitor the protein based or small molecule DNA cleaving agents. Magnetic nanoparticles are used to alter the hydrophobic and hydrophilic properties of electrodes which have applications in studying the electrical properties of electrodes (Katz 2005). In this technique magnetite nanoparticles are functionalized with undecanoic acid which acts as a hydrophobic capping layer. These nanoparticles are suspended in a two-phase system consisting of an aqueous solution and a toluene phase. The attraction and retraction of nanoparticles using an external magnet is used to change the electrode surface to hydrophobic and hydrophilic respectively. Chang's group used magnetite nanoparticles to remove the heavy metal ions in solution (Chang 2005). The nanoparticles are functionalized with carboxymethylated chitosan using carbodiimide and suspended in aqueous solution of Cu (II) ions. The ions will be adsorbed to the nanoparticles surface by changing the pH of solution. The nontoxic nature of PEG modified nanoparticles have applications in more efficient drug delivery compared to the unmodified nanoparticles (Gupta 2004).

Silica coated magnetite nanoparticles have applications in magnetic targeted radiotherapy (Cao 2004). Nanoparticles are modified with N-[3-(trimethoxysilyl) propyl]-ethylenediamine (SG-Si9000) which covalently binds to histidine using glutaraldehyde cross-linker. After that nanoparticles are radiolabeled with ^{188}Re which are used in magnetic targeted radiotherapy.

Polyamidoamine (PAMAM) dendrimer modified magnetite nanoparticles are used to improve the efficiency of protein immobilization (Pan 2005). First aminopropyltrimethoxysilane (APTS) is immobilized on nanoparticles. After that methylacrylate and ethylenediamine are added to form a dendritic structure on nanoparticles surface. Results showed that PAMAM dendrimer coated magnetite nanoparticles are 3.9-7.7 times more efficient than aminosilane modified magnetite nanoparticles. Protein separation is possible with magnetic nanoparticles (Bucak 2003). Phospholipids functionalized nanoparticles acts as ion exchange media to recover and separate proteins from protein mixtures. Sahoo's group synthesized dye-functionalized magnetite nanoparticles that can serve as fluorescent markers (Sahoo 2005). Magnetite nanoparticles having spherical silica nanoparticles doped with protein are used to increase the activity of the entrapped proteins (Yang 2004).

1.2 Self-assembled Monolayers

1.2.1 Background

The term self-assembled monolayers (SAMs) generally represents a monomolecular thick film of organic compounds on flat metal surfaces. They are formed through strong chemisorption between the substrate tail group and the metal surface, leaving the head group free for functionalization to different compounds. This is one of

the basic applications of SAMs in biosensing and other applications. Long-chain alkane thiols form more well-ordered defect-free monolayers than do short chain alkane thiols (Pradier, 2002), additionally the presence of functional groups such as amines, sulphides, selenides provide improved stability (Aslam 2001; Bandyopadhyay 1997; Venkataramanan 1999; Edinger 1993). SAMs can be prepared at room temperature in the laboratory by simply dipping the desired substrate in the required millimolar solution for a specific period of time followed by rinsing with the same solution, water, ethanol and drying using a jet of dry nitrogen. The quality of monolayers depends on several factors such as nature and roughness of the substrate, solvent used, temperature, concentration of the adsorbate (Mourougou-Candoni 2003).

Figure 5 shows the different types of commonly used functional groups and surfaces in the preparation of SAMs.

| Group | Name | Surface |
|--|------------------|---------------------|
| $\text{R}-\text{S}-\text{H}$ | Thiol | Au, Ag, Fe, Cu |
| $\begin{array}{c} \text{O} \\ \parallel \\ \text{R}-\text{C}-\text{OH} \end{array}$ | Carboxylic acids | Metal oxides |
| $\begin{array}{c} \text{Me} \\ \parallel \\ \text{R}-\text{P}-\text{OH} \\ \parallel \\ \text{Me} \end{array}$ | Siloxanes | Metal oxides, glass |

Figure 5. Different Attachment Groups and Substrates for the Formation of SAMs.

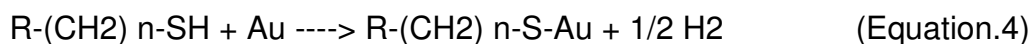
1.2.2 Preparation of SAMs

Organosulphur SAMs can be prepared by immersing gold substrates in millimolar solution of the thiol, sulphide or disulphide. Although it is easy to prepare such SAMs, the quality of SAMs can be improved by considering factors such as roughness of the gold surface, and purity of the thiol solution. The roughness and cleanliness of the glass substrate play an important role while depositing gold. Optically flat glass surfaces are advantageous because of less substrate-induced roughness and lattice imperfections of the gold film. Cleanliness is also paramount; for instance, the glass substrates in this study were cleaned for 1hr in a mixture of water, ammonium hydroxide and hydrogen peroxide (20:4:4 by volume heated about 70°C). The adhesion of gold to glass is very inefficient. Predeposition of a thin chromium or titanium layer on glass can improve the adhesion capacity of gold to glass. Titanium has an additional advantage of having a low diffusion constant. Whereas copper has very high diffusion constant, this will penetrate through the gold layer after a few days. The advantage of gold films is that they can be prepared in large batches and stored over long periods of time. Gold substrates should go directly into freshly prepared thiol solution right after cleaning (Zimmermann 1994).

1.2.3 Characterization of Self-assembled Monolayers

One of the important factors to consider while designing novel biomaterial surfaces with SAMs is the minimization of non-specific adsorption of proteins. It is important to pattern metal surfaces at specific areas for designed functionalization. By coating the metal surface with a protein-resistant polymer it is possible to minimize non-specific adsorption. PEG (poly ethylene glycol) is widely used for preparing protein

resistant surfaces (Tosatti, 2003; Elbert 1996; Brannon-Peppas 2000). Short oligomers of the ethylene glycol alkane thiol monolayers such as HS (CH₂)₁₁(OCH₂CH₂)_n, where n=2-7, prevent the adsorption of most proteins to surfaces (Prime 1993; Mrksich 1995; Zhang 2001). Jeon and Margaret observed that modifications of surfaces with long PEG chains resist protein adsorption via steric stabilization- proteins adsorbed on the surface would cause the glycol chains to compress, which resists the adsorption by desolvating glycol chains (Jeon 1991; Margaret V 1997). Low molecular weight PEG does not readily adsorb onto surfaces. Grafting to the surface is a technique used to form a layer of sufficiently high surface density to achieve protein resistance (Heuberger 2005). While PEG is the most common polymer used to limit non-specific binding, others have been reported, such as gold-tethered polyamine monolayer that was used to reduce the number of adherent bacteria by a factor of 100 compared to bare gold and by a factor of 10 compared to traditional bacterial-resistant polyurethane (Chapman 2001). The assumed formation of a gold–thiolate bond is:



The covalent bond between gold and sulphur has bond strength of 40–45kcal/mol (Whitesides 1990) which contributes to stability of SAMs. Alkane thiols having 12 or more carbons form well-ordered and dense monolayers on gold surface. The thiols attaches to the threefold hollow sites of the gold by losing a proton and forming a hexagonal lattice of thiol molecules (Dubois 1992; Delamarche 1996; Ulman 1996; Balzer 1997). Usually alkane thiols on gold are formed in such a way that they make an angle of 30° (Ulman 1996) to the surface normal. The possible reason is due to tetrahedral bonding between gold, sulphur and the intermolecular interactions of the

thiols in the monolayer. But the length and nature of the end group of thiol determines the angle of tilt with the surface and the extent of motion within the monolayer itself (Wink 1997). For example if the end group is amine or hydroxyl (NH_2 , OH), alkanethiols are densely packed, highly oriented and ordered (Chidsey 1990). On the other hand, COOH and ferrocene groups decrease the density of packing and ordering (Chidsey 1990; Walczak 1991). The nature of the tail group has different applications in immobilizing biomolecules. For example amine-terminated alkaline thiols bind to NHS esters. The active esters are then used to immobilize a protein (Yan 1993; Yan 1994). The $-\text{OH}$ and $-\text{COOH}$ terminates monolayers are useful in wettability studies of different surfaces (Callow 2000). In this project biotin-terminated thiols have used to bind streptavidin conjugated magnetic nanoparticles.

1.2.4 Applications of Self-assembled Monolayers

Self-assembly is a simple chemisorption process that results in strong adhesion to the metal surface and as such, has many applications. It is possible to form self assembled monolayers on different shaped substrates. Depends on the type of adsorbate, control of film thickness is possible at the nanometer level. Most characteristics of the substrates will not get altered except the hydrophilicity of the surface (Jennings, 1998). Organic monolayers formed on the metal surfaces act as a hydrophobic barrier layer, effectively blocking the corrosive ions coming into contact with the metal surface. The defects present in the monolayer allow electrons to pass through, and make it act as a leaky capacitor (Li 2004). Patterned surfaces can be produced at nano-scale levels by photolithography techniques used to pattern gold structures on glass slides. Monolayers having different charges can be formed on these

gold substrates (Tien 1997). SAMs are also useful in generating nanoscale functional structures which have applications in fabrication of electrical circuitry, electronic devices and optical materials (Boncheva 2003; Voldman 1999). SAMs have been used in a robust biosensor based on the quartz crystal microbalance technique to detect antigens. In this technique SAMs are coupled to antibodies via NHS/EDC chemistry. Bovine serum albumin is used to block the non-specific binding sites. High-throughput detection of different antigen-antibody binding events is possible with the functionalized quartz crystal microbalance (Shumaker-Parry 2004). Streptavidin can be used as a linker between a biotin- terminated self-assembled monolayers and biotinylated double stranded DNA, which produces arrays with high packing density. The ideal streptavidin layer provides 5×10^{12} binding sites/cm² for biotin. This allows the dense immobilization of different biotinylated molecules.

SAM's can also be used as ultrathin filters for chemical sensors (Mirsky 2002). Adsorption of mercury, water, iodine and sulphuric compounds on gold surface decreases the conductivity of the gold film. Self-assembled monolayers of hexadecanethiol are used to block the effects of water and volatile sulphuric compounds on the lateral conductivity of the gold layers. They are also used in the passivation of semiconductor surfaces (Hou 1997). GaAs surfaces can be passivated by forming a monolayer of octadecylthiol. Surface passivation also has applications in micro-technology, especially wire bonding. IC circuits use wire bonding to communicate with the outside world. Self-assembled monolayers enable Copper (Cu) to be used for wire bonding. The Cu substrates oxidize rapidly at normal wire bonding temperatures (150-

250°C). SAMs of 1-decanethiol are used to convert CuO to subsequent passivating thiol film (Whelan 2004).

1.2.5 Biotin-SAM's

The binding system plays an important role in an effective immobilization of biomolecules. Biotin-streptavidin system is one of the most well known and frequently used systems. Because streptavidin has four binding sites, bridging of different biotinylated proteins is possible. Streptavidin can be covalently coupled with different ligands such as fluorochromes, enzymes and other tethers which make the biotin-streptavidin system widely used in the study of a variety of biological structures and processes. The availability of wide variety of biotinylated compounds makes the streptavidin/biotin binding pair highly suitable for the molecular recognition at solid surfaces. The pair is useful in biosensor development where one of the couple, often the biotin molecule, is immobilized on the transducer element. Biotin should be immobilized in such a way as to keep maximum biochemical activity and minimum non-specific adsorptions. Biotin can be immobilized onto a gold substrate in two ways, chemisorption and crosslinking. Direct chemisorption of a biotinylated thiol or disulphide is spontaneous, done by immersing clean gold substrates into solutions of biotinylated or disulphides. Cross-linkers can be used to immobilize biotin to gold substrate. First a thiol with an adequate terminal functional group is immobilized on gold, followed by the chemical coupling of an appropriate biotin derivative (Pradier 2002). For example Riepl's group used N,N,NN-tetrame-thyl-(O)-(N-succinimidyl) uronium tetrafluoroborate (TSTU) to activate the carboxylic groups of 16-mercaptohexadecanoic acid, which

binds to the amine groups of the biotin compound (Riepl 2002). Here the carboxylic group was used as a crosslinking functional group.

Pradier's group used TSTU to activate the amine groups of the amine terminated thiol immobilized on gold surface (Pradier 2002). Later the activated amine groups were used to bind to the carboxylic groups of the biotin compound using standard EDC chemistry. The biotin-streptavidin couple was used for specific antigen detection. Streptavidin bound to the silicon substrate was functionalized with NHS biotin (Orth 2003). As streptavidin has four binding sites for biotin, antibodies having biotin binds to the remaining sites of streptavidin to form the couple.

Spinke's group immobilized different biotin terminated thiols on gold and characterized the surface using surface plasmon resonance (Spinke 1993). They found that by increasing the space between the head and tail groups of the thiol, the nonspecific interactions between streptavidin and the surface can be reduced. Also the specific binding between streptavidin and biotin groups can be increased. Pradier's group used bovine serum albumin (BSA) to reduce the nonspecific binding of avidin to the gold surface (Pradier 2002). Fritzsche's group demonstrated the specific interaction between biotin and streptavidin using wet-masking technique (Fritzsche 1998). In this technique, first a self-assembled monolayer of biotin-HPDP was formed on gold substrate. After that part of the slide is covered with silicone elastomere Sylgard 182 having a thickness of 1-2mm. after that streptavidin was bounded to the biotin in the uncovered areas of the substrate. The slides were characterized using scanning force microscopy (SFM). Shumaker-Parry's group used the biotin-streptavidin couple to study protein-DNA interactions (Shumaker-Parry 2004). Surface plasmon resonance

(SPR) was used to characterize the functionalized gold surface. Gau's group fabricated a microelectromechanical systems (MEMS) based biosensor to detect E.Coli bacteria which uses biotin-streptavidin couple in the detection (Gau 2001). Results showed that a biotinylated thiol SAM gives better results compared to the direct adsorption of streptavidin on gold.

In this study biotin-HPDP and sulpho NHS-biotin are used for capture of streptavidin-conjugated nanoparticles which has future applications in biosensing. The SAM modified surfaces were characterized using various techniques described in the following section.

1.3 Characterization Techniques

1.3.1 Transmission Electron Microscopy (TEM) and Scanning Electron Microscopy (SEM)

TEM and SEM use electrons instead of light waves to generate magnified images. Both use magnetic lenses to deflect the electron beam. In TEM the electrons are passed through the sample and the resulting pattern of electron reflection and absorption is magnified on a fluorescent screen, whereas in SEM the electrons are reflected from the sample surface and the secondary electrons or X-rays emitted from the sample surfaces are detected by the detector. Due to this fact the resolution of images from TEM is higher than that of SEM. For the TEM sample preparation, a drop of sample is placed on a carbon coated copper grid, left overnight in the dark, and dried with a heat gun. Alternatively, a drop of sample solution can be attached on one side of the copper grid, which is then gently placed on filter paper with the opposite site facing down. As SEM uses reflection properties of surface for imaging, imaging of materials bounded to solid surfaces is possible. First the surface is coated with a conducting layer

such as gold, copper and then exposed to the jet of electrons for imaging. In this study TEM was used to measure the size of nanoparticles and SEM was used to confirm the binding of nanoparticles to gold surface.

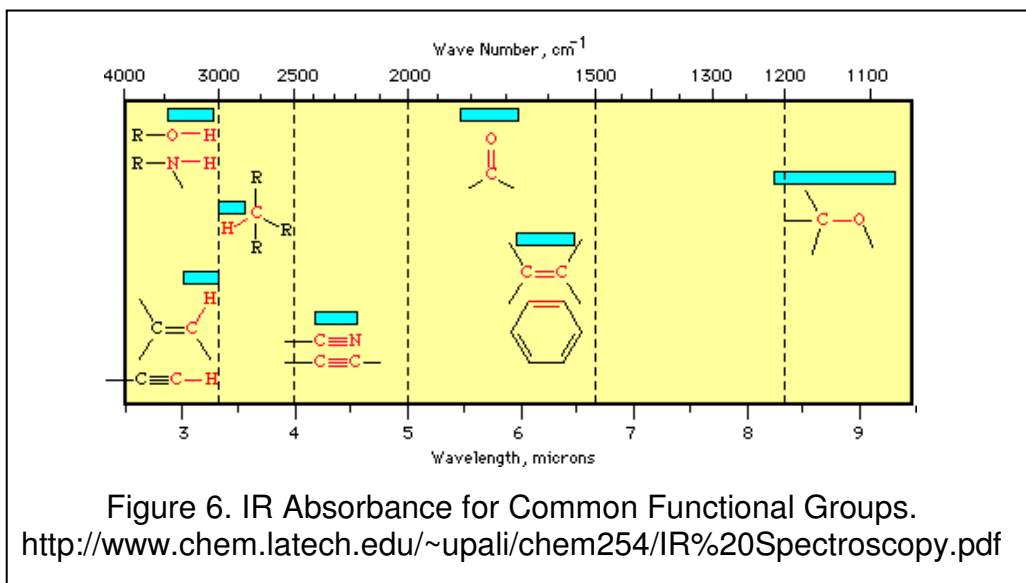
1.3.2 Energy Dispersive X-ray Spectrometry (EDS)

It is often necessary to identify the different elements associated with a specimen. SEM combined with a built-in spectrometer called an Energy Dispersive X-ray Spectrometer is used for this purpose. In this study EDS analysis was used to confirm the composition of particles immobilized on gold surface. EDS is an analytical technique which utilizes X-rays that are emitted from the specimen when bombarded by the electron beam to identify the elemental composition of the specimen. The electron beam encountering the material generates X-rays characteristic of the different elements present. These X-rays can be detected by an additional detector attached to the SEM. The analysis of the chemical composition of small details found in SEM images by EDS is extremely useful in most metallographic and biomaterial studies. EDS can provide rapid qualitative, or with adequate standards, quantitative analysis of elemental composition within a sampling depth of 1-2 microns.

1.3.3 Fourier Transform Infrared Spectroscopy (FT-IR)

Identification of specific types of chemical bonds or functional groups based on their unique absorption signatures is possible by infrared spectroscopy. Figure 6 shows the infrared absorbance of common functional groups that are present in chemical compounds. Alcohols produce infrared bands due to O-H stretching centered at 3600cm^{-1} . Different types of amines can be differentiated by using infrared spectra. Primary amines show two characteristic N-H stretching bands near 3335cm^{-1} whereas

secondary amines show only one. Secondary amines also show an N-H bending band at 1615 cm^{-1} . The N-CH₂ stretching band at 2780 cm^{-1} is due to the presence of tertiary amines in the compound. The C-H bonds in aldehydes have a characteristic stretching band centered at $2700\text{-}1900\text{ cm}^{-1}$. The peaks centered at $1740\text{-}1720\text{ cm}^{-1}$ and $1720\text{-}1680\text{ cm}^{-1}$ are due to the carbonyl stretching of aliphatic and aromatic aldehydes respectively. Alkenes containing the C=C group have two major bands. First, the =C-H stretching between $3100\text{-}3000\text{ cm}^{-1}$ and C=C stretching between $1600\text{-}1430\text{ cm}^{-1}$. The stretching absorptions of triple bond between carbon and nitrogen occur between 2400 and 2200 cm^{-1} .



1.3.4 Reflection Absorption Infrared Spectroscopy(RAIRS)

Reflection-Absorption Infrared Spectroscopy (RAIRS) is a special type of FT-IR which is used to generate absorption as well as reflection bands. It is widely used to characterize metal surfaces having absorbents. When molecules are adsorbed to a surface the bonds between different atoms will vibrate. The frequency of these vibrations can be measured by shining infrared light onto the surface. Molecules having

a dipole moment can absorb infrared light which gives rise to missing absorption bands. RAIRS is used to acquire information about these missing absorption bands. Vibrations can only be detected if the vibration is perpendicular to the surface (Trenary 2000).

1.3.5 Fluorescent Microscopy

Fluorescence is a rapid process of emission of light of longer wavelength from a material when it absorbs a light of given wavelength. The fluorescence process occurs in certain molecules called fluorophores or fluorescent dyes. Different fluorescent probes can be attached to the biological specimens who can emit light when they absorb a specific wavelength of light. This procedure is extremely rapid and takes only 10^{-12} seconds. Different fluorescent molecule possesses different characteristic absorption and emission spectra. A fluorescent microscope consists of a light source (usually a mercury lamp), a filter which enables only a certain wavelength to pass, a microscope objective to project a diffraction-limited image at a fixed plane, and a dichroic mirror which reflects light shorter than a certain wavelength, and passes light longer than that wavelength and a emission filter used to select the emission wavelength of the light emitted from the sample and to remove traces of excitation light. In this study fluorescent microscopy was used to image the captured nanoparticles on the gold surface.

1.3 6 X-ray Photoelectron Spectroscopy

The photoelectric effect leads to the production of photoelectrons that are emitted if the energy of the absorbed photons is high enough. Excess energy is transferred to the electron as kinetic energy. The binding energy is determined by the difference between the energy of the incident photon and the kinetic energy of the

emitted electron. High energy X-rays are required to study the properties of core electrons of the atom. X-ray photoelectron spectroscopy (XPS) consists of a source of fixed energy radiation to emit X-rays. A monochromatic source must be used to get high energy X-rays. The source should have multiple-anode handling capacity and high lifetime. An electron energy analyzer is used to disperse the emitted electrons based on their kinetic energy, and measure the flux of emitted electrons of a particular energy. It requires precision energy measurements over a wide range of bond energies of elements and ability to define the analysis area. Clean vacuum pumps operating at a base pressure 10^{-10} torr (10^{-8} Pa) are required to remove the adsorbed gases from the sample, to increase the mean free path for electrons analyzer, to improve the efficiency of the X-ray and electron optics. In this study XPS was used to confirm the binding of biotin to the gold surface.

Chapter 2

Functionalization and Characterization of Gold and Glass Surfaces

2.1 Introduction

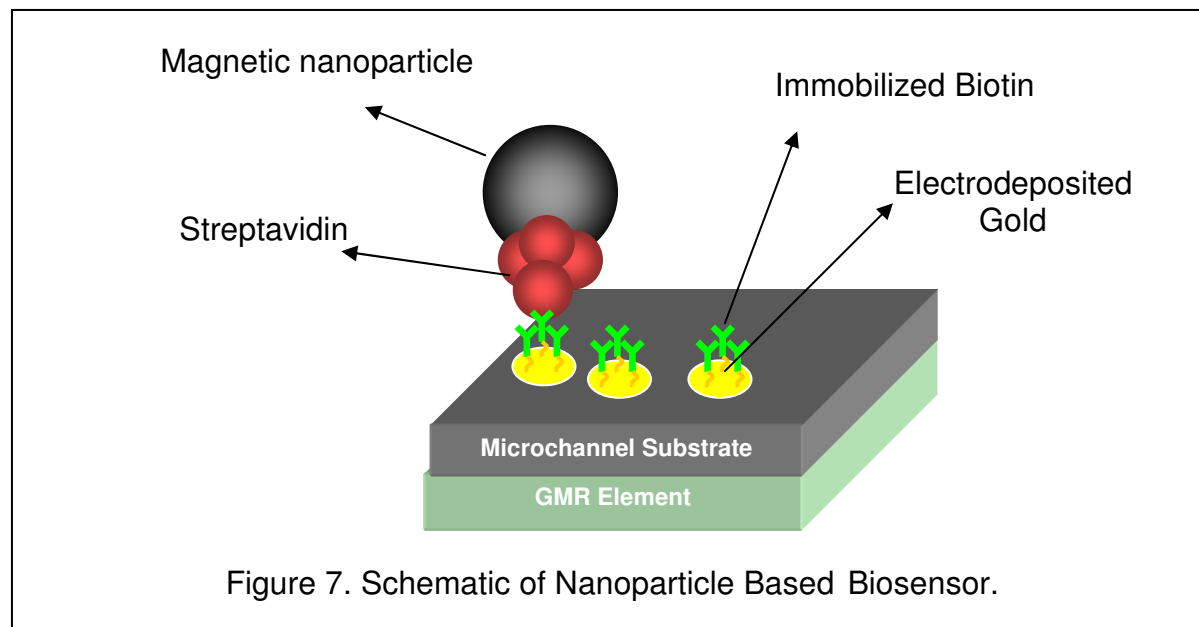
Over the past few decades, the study of magnetizable objects in the nanometer scale has generated considerable interest in scientific applications. They have influenced detection and imaging processes such as magnetic resonance imaging (Artemov 2003), protein detection (Cao 2003; Bucak 2003), and molecular and cellular separation and purification (Molday 1982; Yang 2004). They also have applications in increasing efficiency in site-specific drug delivery (Forbes 2003; Lubbe 2001), cancer treatment (Hilger, 2004; Zhang 2005), and in increasing enzymatic activity (Kouassi 2005; Rossi 2004; Pan 2005). Various types of nanoparticles are being used in biosensing schemes to show improvements over microparticles. Nanoparticles have several advantages in detecting biological molecules compared to microparticles, such as high magnetization per unit weight, ability to remain in suspension for longer periods of time without aggregation, and faster velocities in solution (Moller 2003). Functionalization of magnetic beads with biological recognition elements that can bind to specific targets has several advantages in the detection of biomolecules compared to radioactive, electrochemical, optical, and other methods (Rife 2003). For example, radioimmunoassay requires expensive instrumentation and handling of potentially hazardous radioactive materials; whereas, magnetic bead detection is cheap, efficient, and safe. Biomedical applications using nanoparticles require narrow size distribution and compatibility with surface modifiers i.e., nonimmunogenic, nonantigenic and resistant to protein adsorption (Pankhurst 2003). Here we demonstrate the synthesis

and functionalization of nanoparticles that could be utilized in any of these aforementioned applications.

The recognition and capture of molecules and particles at solid surfaces has numerous bioanalytical applications in bio- and immunosensor diagnostic devices (Yam 2002). The immobilization of bio-recognition molecules, such as nucleic acids, proteins and other ligands on solid surfaces plays an important role in the development of such devices. For efficient immobilization, the maximum biochemical activity and minimum nonspecific interactions must be achieved. Using a system that couples proteins with nanoparticles, the efficiency of the immobilization can be increased. Here we demonstrate a system for functionalization of magnetic nanoparticles in addition to functionalized surfaces for their binding in an effort to move towards nanoparticle based bio-recognition schemes.

The biotin and streptavidin couple is an ideal model for these types of bioconjugation applications because of its high binding affinity ($K_a=10^{15} \text{ M}^{-1}$) and high specificity (Yam 2002). These properties enable streptavidin to act as a bridge between immobilized biotinylated moiety and the detectable nanoparticles. Each streptavidin has four binding sites for biotin positioned in pairs on opposite domains of the protein molecule. Nanoparticle-protein binding occurs between the amine residues on the nanoparticle surface and the carbodiimide-activated carboxylic group of streptavidin (Kumar 2004). Several forms of commercially available thiolated biotin can be immobilized to gold surfaces via sulphur linkages have been evaluated (Pradier 2002). The high affinity of gold for sulphur-containing molecules generates well-ordered monolayers termed self-assembled monolayers (SAMs). In this ongoing effort we

describe the synthesis of streptavidin-functionalized magnetic nanoparticles and characterize their binding to biotinylated SAMs on gold for biological recognition applications. Figure 7 shows a schematic of such a magnetic nanoparticle based biosensor, whereby biomolecular interaction is detected by a change in resistance from a GMR element when a functionalized nanoparticle binds to the immobilized target.



The study has been divided into three parts: part one consists of the synthesis and functionalization of nanoparticles, part two consists of the functionalization of gold and glass surfaces with thiolated biotin, and part three consists of specifically binding of the functionalized particles onto the biotinylated gold surface. In each part, functionalization is confirmed using various imaging and spectroscopy techniques. Because nanoparticles have increasing applications in magnetic bio-sensing, the ability to functionalize them and the surfaces to which they bind is necessary for the fabrication of future GMR based biosensors based on nanoparticles.

2.2 Material and Methods

Immobilization of different types of thiolated biotins on to the gold substrates was achieved by the strong covalent linkage between sulphur and gold. Biotin-HPDP and Sulpho NHS-biotin were used to functionalize gold surface and glass surface. Biotin-HPDP has an advantage of having a self-spacer pyridine 2-thiol which is generated by the reduction of Biotin-HPDP with butyl phosphine. Cleaning of the gold substrate plays an important role in immobilizing biotin on gold. The gold substrates were stored in ethanol upon arrival because of the presence of titanium which diffuses when exposed to the atmosphere for long times, and also to avoid oxidization of gold surface. Freshly prepared solutions of thiols were used for an effective functionalization of gold surface. The advantage of Sulpho NHS-biotin is its water-soluble capacity and ability to bind to aminated glass substrates through NHS chemistry. The gold substrates were functionalized with biotin-HPDP by dipping the gold slide into the freshly prepared millimolar solution of biotin-HPDP. Aminated glass substrates were functionalized with sulpho-NHS biotin by spotting a solution of NHS biotin using a microcapillary.

Glass substrates having 50A^o chromium base layer and a 1000A^o evaporated gold film were purchased from EMF Corporation. Biotin-HPDP, sulpho-NHS biotin (Pierce Biotechnologies), fluorescein-5-isothiocyanate (FITC) labeled streptavidin (Molecular Probes), and tributyl phosphine, N, N-dimethyl formamide (DMF, Sigma), superamine substrates (ARrayit) were used as received.

2.2.1 Synthesis of Nanoparticles

Iron oxide magnetic nanoparticles (Fe₃O₄) were prepared by co-precipitating Fe⁺² and Fe⁺³ ions by ammonia solution. Ferric and ferrous chlorides were weighed in

an inert atmosphere (e.g., a glove box) because of their high oxidizing capacity. The ferric and ferrous chlorides were dissolved in nanopure water at a concentration of 0.3 M iron ions. Chemical precipitation was achieved at 25°C under vigorous stirring by adding NH₄OH solution. A pH of 10 was maintained during the synthesis process to reduce ferrous and ferric chlorides. The precipitants were heated at 80 °C for 30 minutes, washed three times with water and once with 100% ethanol, and dried under nitrogen (**Kumar 2004**). No surfactant was used in the nanoparticle synthesis process.

2.2.2 Functionalization of Nanoparticles with Streptavidin

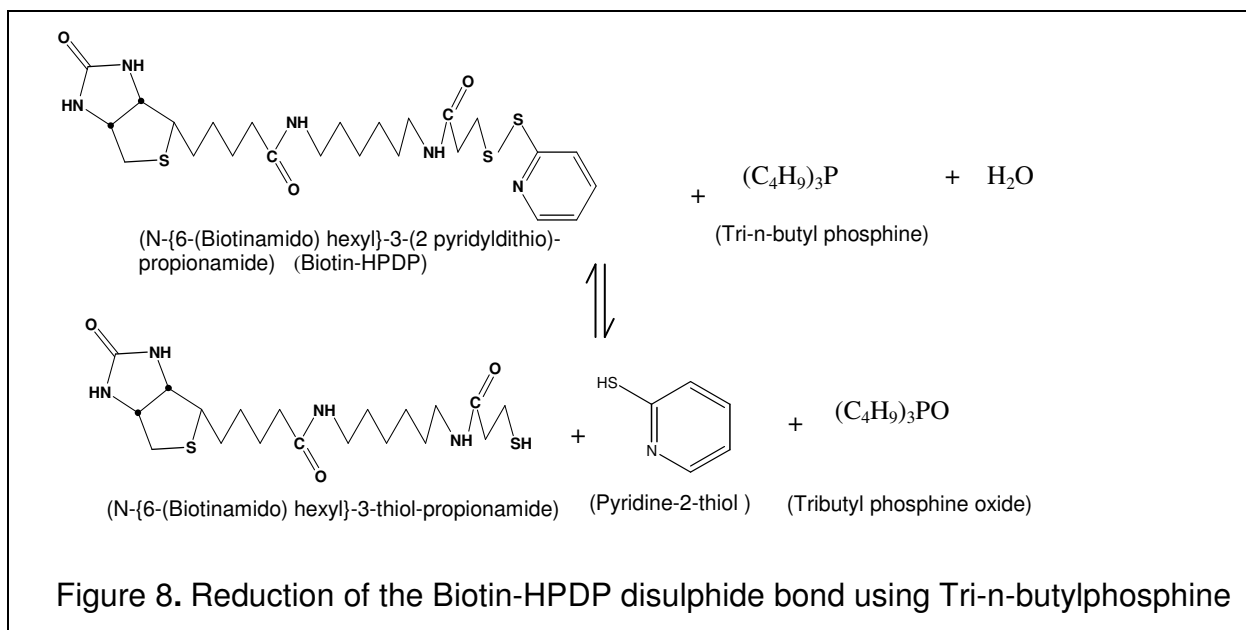
Functionalization of nanoparticles with FITC-streptavidin was achieved by carbodiimide chemistry, similar to that of enzyme binding to nanoparticles (Kumar 2004). 5 mg of the magnetite particles was added to 0.3 ml of water and sonicated for 10 minutes after addition of 5 mg of carbodiimide. Finally, 100 µl of streptavidin-FITC solution (1 mg/ml) was then added, and the reaction mixture was sonicated for 30 minutes. This binding process was carried out at a constant temperature of 4°C. The streptavidin-bound nanoparticles were recovered from the reaction mixture with the use of a permanent magnet. The particles were washed with water three times and dried under nitrogen.

2.2.3 Immobilization of Biotin-HPDP on Gold

Gold substrates were heated (70°C) for 30min in a 20:4:4 mixture of water, ammonium hydroxide and hydrogen peroxide, respectively. The surface was then rinsed with water and dried with nitrogen. The slides were then dipped in Nano Strip solution (Cyntec Corporation, Mixture of Sulfuric Acid and Hydrogen Peroxide) for 30

minutes. The gold substrates were then immersed in warm (~70°C) 100% ethanol solution to reduce the gold substrate.

A Biotin-HPDP solution was prepared in a two-step process. First, 1 mg of biotin-HPDP was dissolved in 8 ml of DMF by sonicating at 45°C. After 3 minutes of sonication, 5 µl of butylphosphine solution was added to the solution and reacted for 30 minutes. Butylphosphine was used to reduce the disulphide link of biotin-HPDP to a thiol (detailed in Figure 8), confirmed by a change in solution color from white to yellow. The mixture was next added to 8 ml of (1:1) water and ethanol. The cleaned substrates were dipped in the biotin-HPDP solution for 48 hours. The samples were then washed with water, 100% ethanol and dried with nitrogen and stored in HPLC-grade water until use (Zimmermann 1994).



2.2.4 Binding of Streptavidin to Biotinylated Gold Surfaces

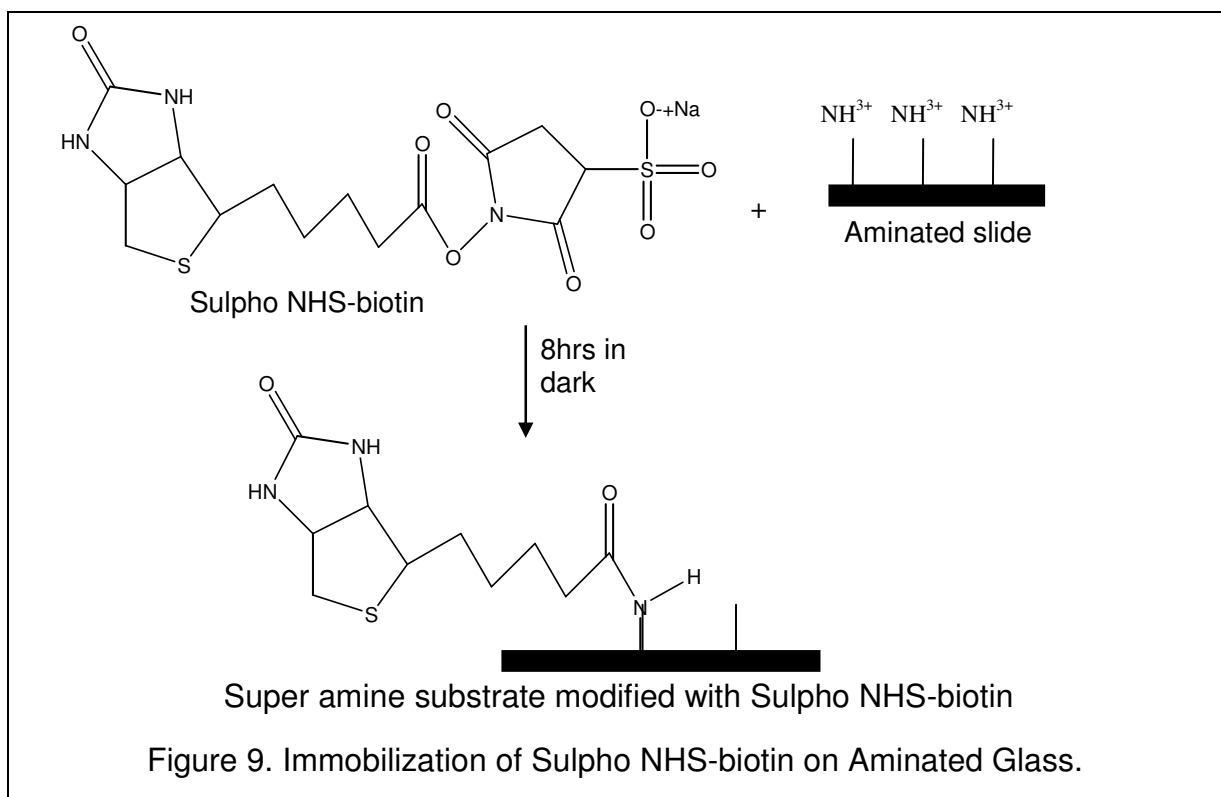
Biotinylated substrates were immersed into a 2 µM solution of FITC-streptavidin in TE buffer (Tris-EDTA, 10 mM, pH 7.5) for three hours, followed by rinsing with HPLC-grade water and finally dried under nitrogen (Zimmermann 1994).

2.2.5 Binding of Streptavidin Conjugated Nanoparticles to Biotinylated Gold surface

Nanoparticle capture was performed by spotting 10 μ l of the nanoparticle solution onto the biotinylated gold surface with a micropipette tip and kept in the dark for 1hr. The substrates were rinsed with HPLC-grade water and dried under nitrogen.

2.2.6 Binding of Sulpho NHS-biotin to Aminated Slide

Sulpho NHS-biotin (10mM) was prepared in HPLC-grade water. The glass substrates were cleaned with water and ethanol, and then dried with nitrogen. Using a microcapillary tube, the thiol solution was deposited onto the amine slide. The slides were kept in dark for 8hrs and washed with HPLC-grade water and ethanol. After that the slides were dried with pure nitrogen. Figure 9 shows the reaction between sulpho NHS-biotin and the aminated glass surface.



2.2.7 Binding of Streptavidin Conjugated Nanoparticles to Biotinylated Glass Surface

Streptavidin conjugated nanoparticle solution (5 μ l) was pipetted onto the glass slide in such a way that it covered the areas of slides with and without biotin. The slides were then kept in the dark for 2hrs, and then washed with DI water and ethanol. After that they were dried with nitrogen.

2.3 Characterization of Functionalized Gold Surfaces

The functionalized gold surface was characterized by transmission electron microscopy (TEM), Fourier transform infrared spectroscopy (FT-IR), fluorescent microscopy, X-ray photoelectron spectroscopy (XPS), and scanning electron microscopy (SEM).

2.3.1 Transmission Electron Microscopy (TEM)

The morphology and size of the particles were examined by a JEOL 100CX transmission electron microscope (TEM) at accelerating voltages up to 80keV. The TEM samples were prepared by placing a drop of iron nanoparticle solution on a holey carbon-coated copper grid. The excess solvent was evaporated under an argon atmosphere and the specimen was dried in a vacuum. Image analysis to determine nanoparticle diameter was performed using ImageJ software (NIH, Bethesda, MD).

2.3.2 Fourier Transform Infrared Spectroscopy (FT-IR)

Infrared spectroscopy was used to collect chemical bonds data present in the SAMs and SAM-nanoparticle complexes. Due to the dipolar nature of the excitations in the infrared, the technique can also provide information about orientation of molecules and molecular entities using polarized light. This feature is of particular importance for SAMs

since it can be employed to determine chain and functional group orientation on the surface. FT-IR spectra were recorded on a NEXUS 670 FT-IR. A wide band HgCdTe detector, cooled with liquid nitrogen, was used to collect the data at 4cm^{-1} resolution. The FT-IR beam was focused onto the sample at an incidence angle of 87° . Purging the system with liquid nitrogen before taking scans eliminated water and CO_2 absorption contributions. A reference spectrum was taken on a clean gold substrate. For all spectra, 500 scans were collected, smoothed by 25 to eliminate the background noise.

2.3.3 Fluorescent Microscopy

Fluorescence images of functionalized gold surfaces were obtained on a TS100 fluorescence microscope (Nikon Eclipse) with a mercury arc lamp source. Filters with excitation wavelengths of $492\pm 10\text{nm}$ and emission wavelengths of $525\pm 10\text{nm}$ were used. Phase and fluorescent images of functionalized nanoparticles immobilized on amine terminated glass substrates are taken at 2X, 5X, 10X, and 40 X magnifications.

2.3.4 X-ray Photoelectron Spectroscopy

X-ray photoelectron spectroscopy spectra were obtained on an Axis 165 spectrometer equipped with a monochromatic AlK α X-ray source. The technique provides information about the core electronic levels in atoms and molecules and has been frequently used to find correlations between the solution and surface (SAM) composition. A takeoff angle of 90° from the surface was employed for each sample. Survey spectra were recorded with 15KeV pass energy of a $300\mu\text{m} \times 800\mu\text{m}$ spot size. A window pass energy of 20eV was used to acquire high-resolution spectra.

2.3.5 Scanning Electron Microscopy (SEM)

SEM coupled with Energy Dispersive Spectrometry (EDS) is a method for high-resolution imaging and elemental characterization of functionalized surfaces with spatial resolution. Hitachi Model S-3600N SEM was used to characterize the functionalized gold surface SAMs and SAM-nanoparticle complexes. The images were taken at 10 μ m and 50 μ m resolution. EDS analysis supports identification of material phase compositions at atomic levels, even for extremely small particles. Image analysis to determine nanoparticle diameter was performed using ImageJ software (NIH, Bethesda, MD).

2.4 Results and Discussion

Transmission electron microscopy (TEM) of magnetic nanoparticles shows that the iron oxide particles dispersed in water have dimensions of 9.8 ± 4.6 nm (Figure 10). Some aggregation of particles was observed most likely because surfactant was not used in this particular synthesis method (Teng 2004; Lu 2004).

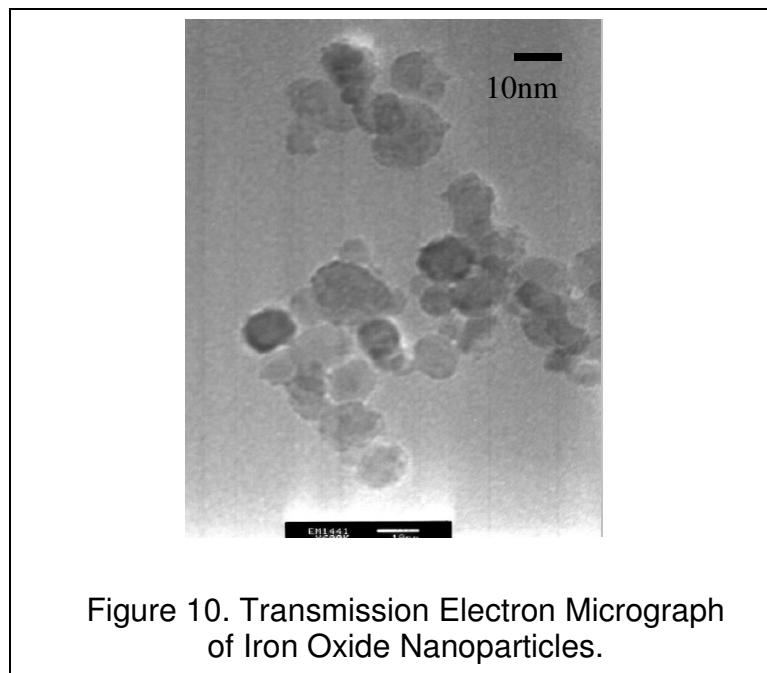
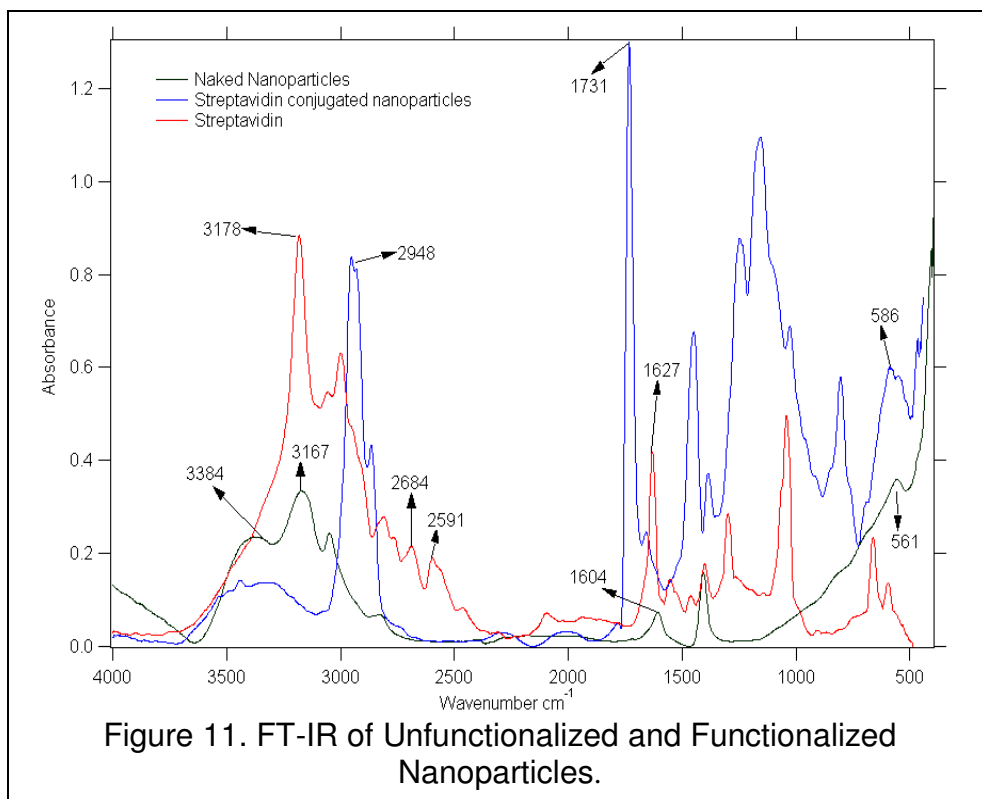


Figure 11 shows the FT-IR spectra of unfunctionalized and functionalized nanoparticles. It also shows the FT-IR spectra of streptavidin deposited onto the gold surface. The characteristic peaks at 3167cm^{-1} and 1604cm^{-1} present in spectra of unfunctionalized particles confirm the presence of amine groups in unfunctionalized nanoparticles. The peak at 561cm^{-1} confirms the presence of magnetite nanoparticles similar to other reports (Waldron 1955; Gupta 2004; Curtis 2002). The same was shifted to 586cm^{-1} after functionalization with streptavidin. The peak at 2948cm^{-1} present in the spectra of functionalized nanoparticles can be attributed to CH_2 stretches, which was not observed in unfunctionalized particle spectra, indicating that the nanoparticles were modified.



FT-IR spectra in Figure 12 confirm the immobilization of biotin-HPDP to the gold surface. The peaks at 2942cm^{-1} were due to the CH_2 stretching vibrations of the

alkyl chain (Pradier 2002). The broad band at 1674 cm^{-1} was due to the amide-1 bands of biotin-HPDP similar to those reported previously with this technique. The band at 3328 cm^{-1} was due to the secondary amide N-H stretching (Pradier 2002). The band at 538 cm^{-1} present in the spectra of deposited biotin was assigned to the disulphide bond of biotin-HPDP. As this S-S bond of biotin-HPDP was reduced, the band disappeared in the spectra of immobilization.

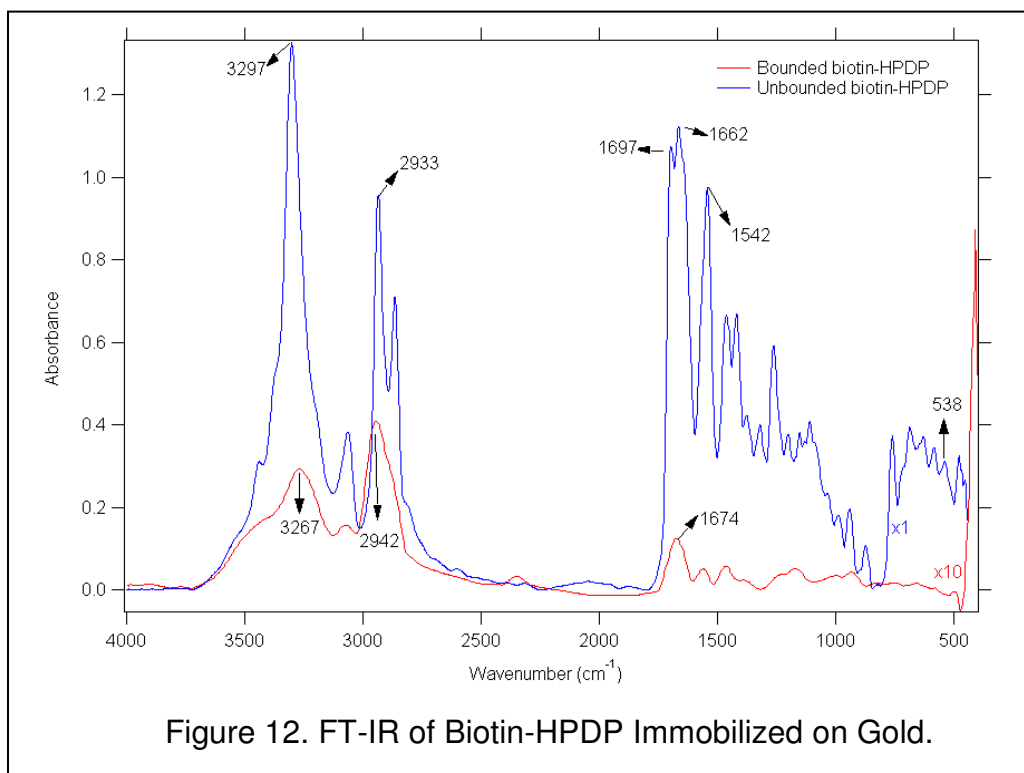
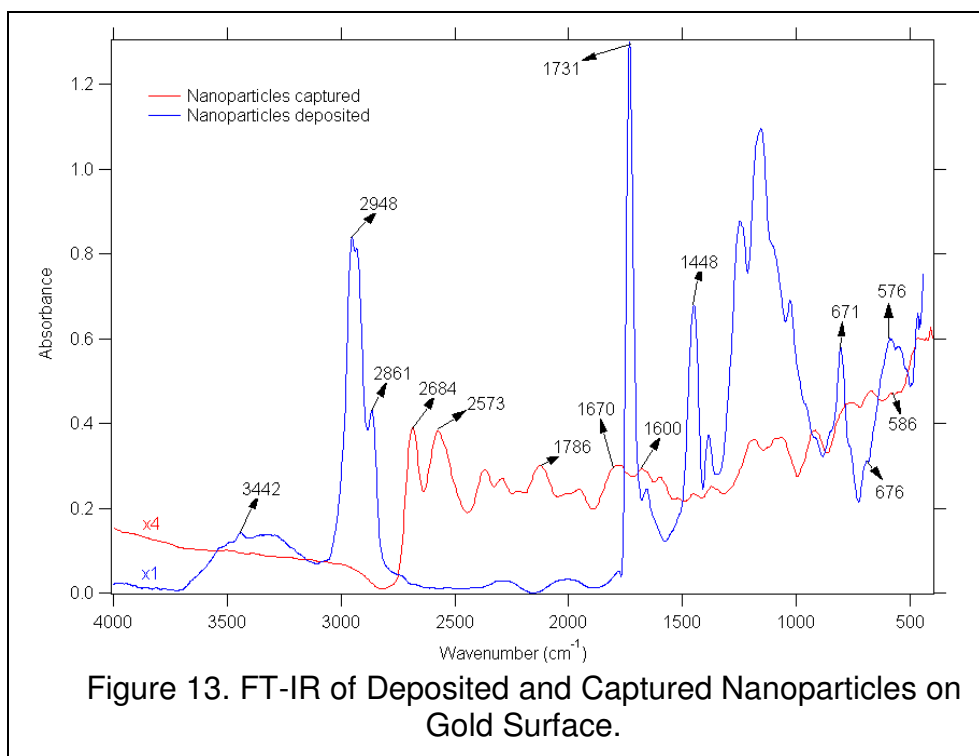
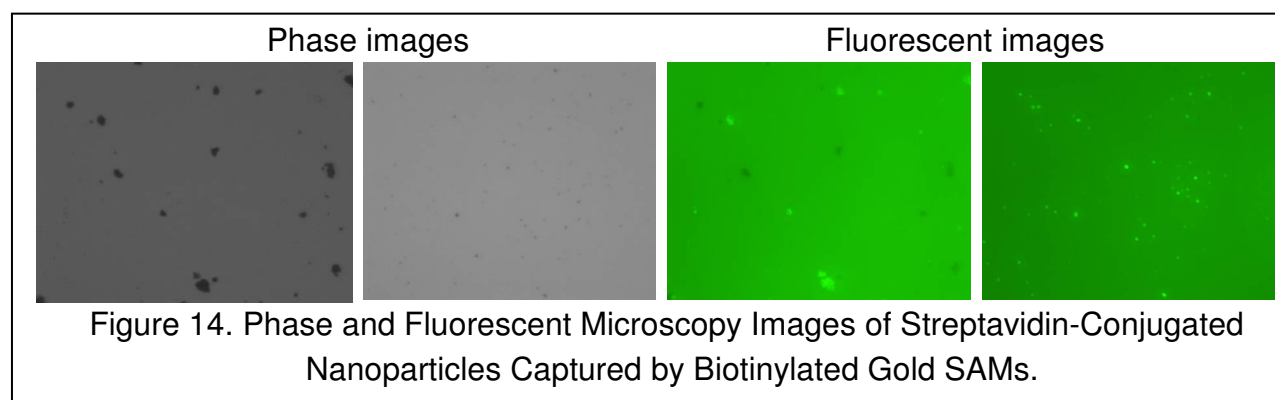


Figure 13 shows FT-IR spectra of the deposited and captured nanoparticles conjugated with streptavidin. A characteristic peak between 576 cm^{-1} was observed in the spectra of deposited nanoparticles (Waldron 1955; Gupta 2004). This is due to the presence of Fe_3O_4 nanoparticles. The peak has been slightly shifted to 586 cm^{-1} after capture by the biotinylated surface, which confirms the presence of nanoparticles immobilized by biomolecular interactions (Chen 2000; Curtis 2002). The peaks at 1600 cm^{-1} and

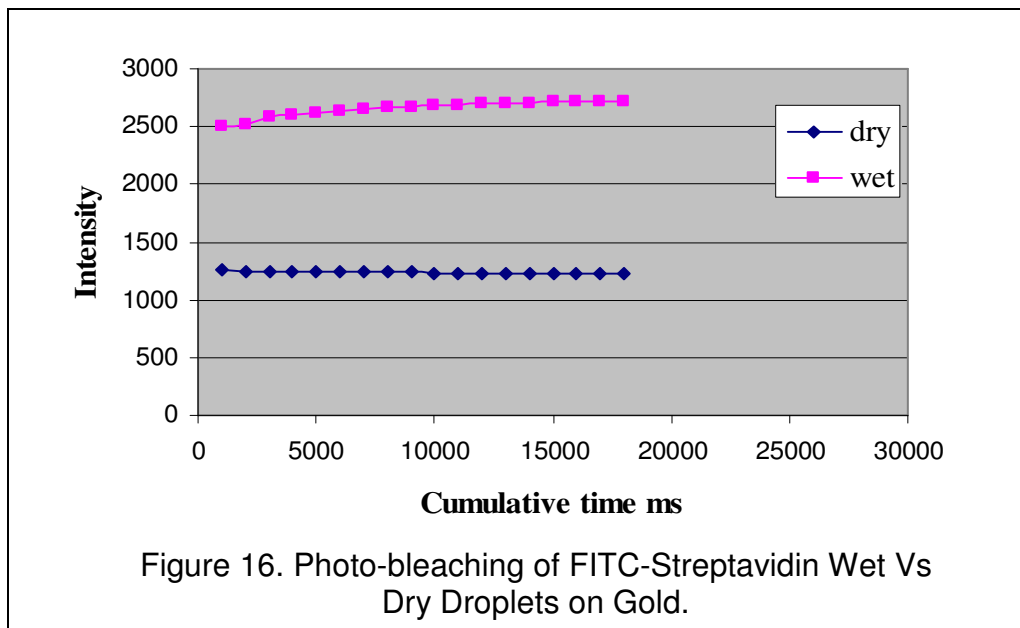
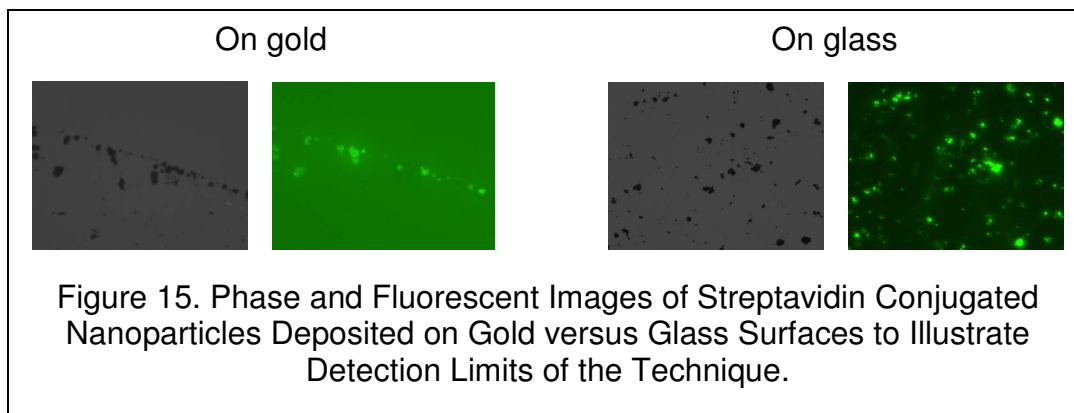
1660 cm^{-1} were due to the amide-I stretches of the N-H groups present in biotin-HPDP on the slide for nanoparticle capture, which was not present on the deposition slide.



Fluorescent images in Figure 14 show that particles are bound to the functionalized gold surface even after extensive washing. Some quenching of fluorescence is observed because of the short distance of the fluorophore-nanoparticle conjugates to the surface of gold. The high reflection of the gold surface also increases the background signal and reduces the sensitivity of this technique's detection limits.



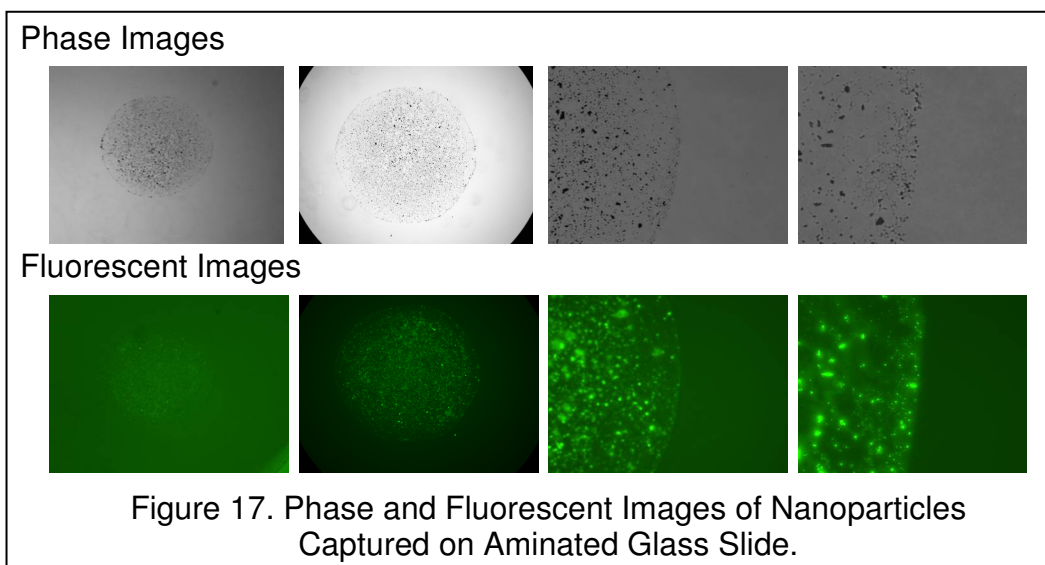
To illustrate the difference in fluorescent signals from gold and standard glass surfaces, streptavidin-conjugated particles were deposited on gold and glass slides containing no biotin. Fluorescent images of both the samples were taken at 40X with an exposure time of 10sec. Low fluorescence of particles observed on gold, suggests quenching when compared to fluorescence on glass slides (Figure 15).



Effect of exposure time on the fluorescence intensity of FITC-streptavidin is shown in figure 16. The percentage changes in the intensity over an 18sec continuous exposure are +16% and -3% relative fluorescence units for wet and dry respectively. This

confirms that FITC-streptavidin does not significantly decrease its fluorescence emission for the exposure times used in this study, and photo bleaching alone does not explain the poor quality of images on gold surfaces with the existing microscope configuration.

Phase and fluorescent images of nanoparticles captured on aminated glass surface are depicted in figure 17. The fluorescent images show the specific absorption of streptavidin conjugated nanoparticles to the biotinylated area of the slide, which was a spot of approximately 1960 μm in diameter.



The carbon 1s, nitrogen 1s, and oxygen 1s atomic orbital spectra were measured with XPS for gold surfaces with and without biotin-HPDP as seen in Figure 18.

It is evident that there was an increase in the intensities of nitrogen, carbon, and oxygen after the functionalization of gold with biotin-HPDP. The carbon 1s peak, at 285.1 eV, was assigned to the CH_2 groups of biotin-HPDP (Riepl 2002). The nitrogen 1s peak at 400.3 eV was assigned to the NH groups of biotin-HPDP (refer to Figure 18). The

oxygen 1s peak centered at 532 eV was due to the increase in the number of oxygen atoms present in biotin-HPDP (Riepl 2002; Pradier 2002).

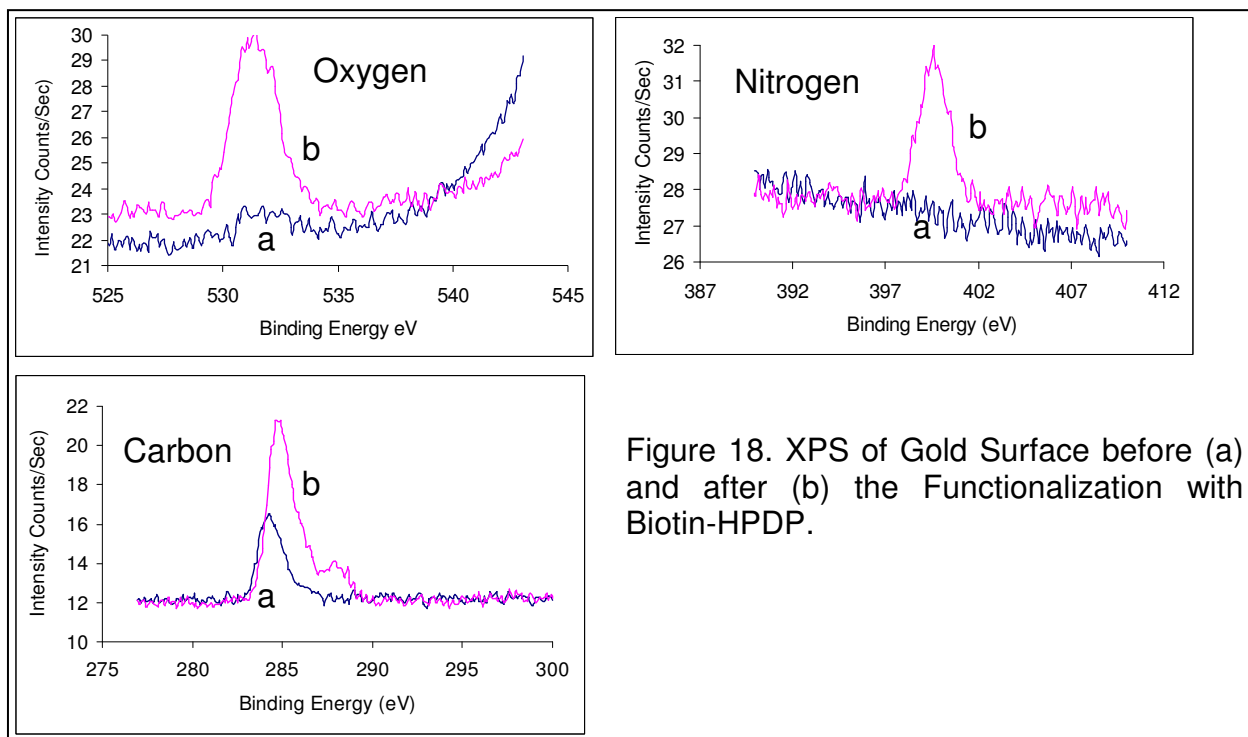
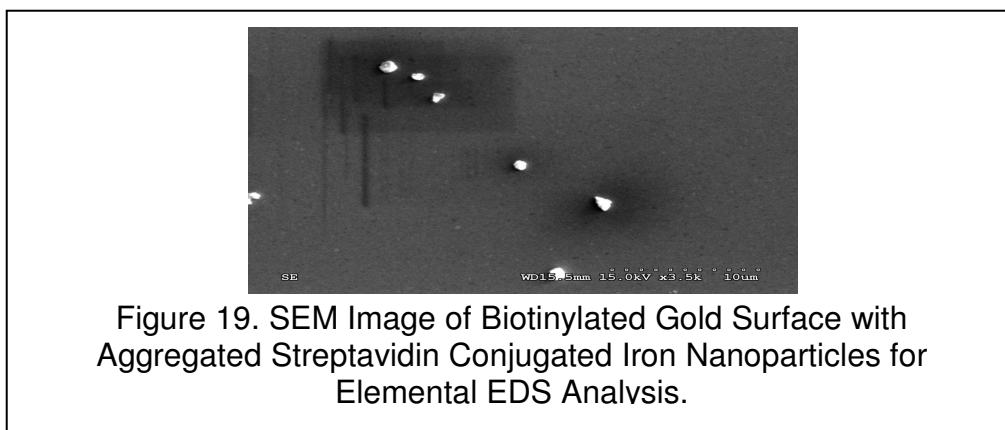


Figure 19 shows a SEM image of nanoparticles bound to the biotinylated gold surface. The size of the particles was not uniform because of some aggregation, but this fact facilitated elemental analysis via EDS. Figure 20 confirms the presence of iron, carbon, and nitrogen, which is consistent with the principle elements found with the attachment of protein-nanoparticle complexes.



Figures 20 A and B show EDS analysis of small and large particles respectively. An increase in the EDS signal of iron (Fe) was observed as the size of the particle increased. There is a higher carbon signal compared to iron observed in the smaller particles. The possible reason for this might be heavily aggregated particles that have less streptavidin bound to them.

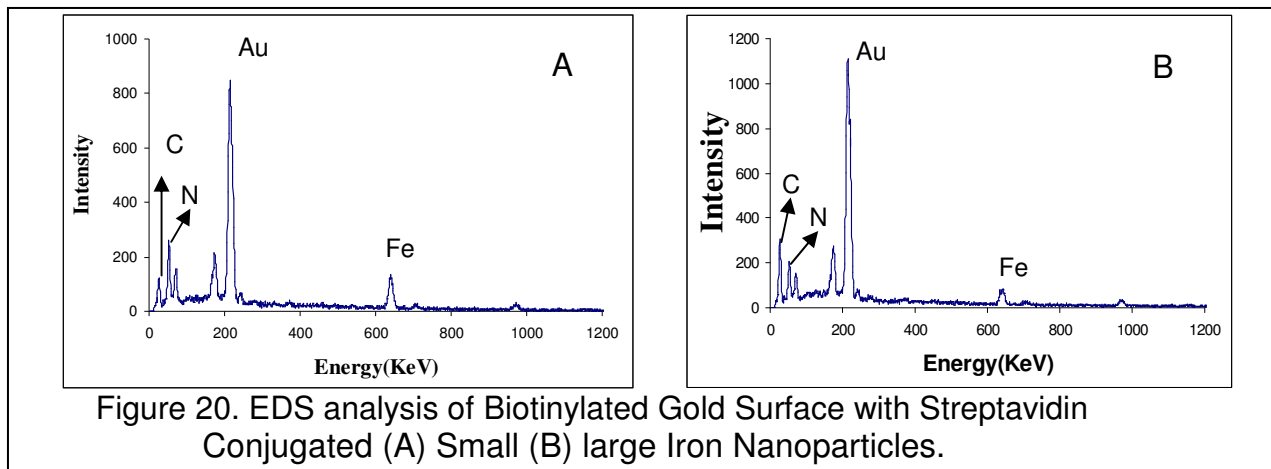
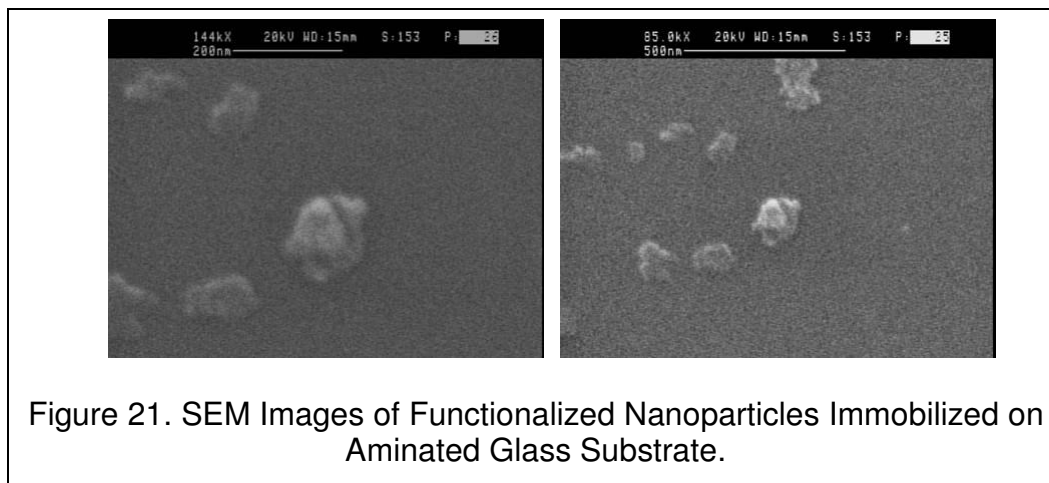


Figure 21 shows SEM images of functionalized nanoparticles immobilized on aminated glass substrate. The slides were scanned at 200nm and 500nm resolution. The results show that particles were aggregated with an average size of $106.58 \pm 46.36 \text{ nm}$.



Immobilization of functionalized nanoparticles on the biotinylated gold surface was achieved by the strong interaction forces between biotin and streptavidin. The nanoparticle functionalized substrates were characterized by SEM, fluorescent microscopy, and FT-IR to show that little capture occurred in non-biotinylated regions of the gold and glass surfaces.

Chapter 3

3. Conclusions and Future Considerations

3.1 Conclusions

In this ongoing effort we describe the synthesis of streptavidin-functionalized magnetic nanoparticles and characterize their binding to biotinylated SAMs on gold for biological recognition applications. Magnetic nanoparticles (Fe_3O_4) were prepared by co-precipitating Fe^{+2} and Fe^{+3} ions by ammonia solution. The TEM analysis indicated the smallest size of the magnetic nanoparticle was in the range of $9.8 \pm 4.6 \text{ nm}$. They also confirmed that particles are aggregated because of their magnetic attractions to each other. FT-IR data confirmed that the particles were successfully conjugated to streptavidin. XPS analysis showed an increase in the intensity of carbon 1s, nitrogen 1s, and oxygen 1s peaks after gold surface was functionalized with biotin-HPDP. FT-IR data confirmed the immobilization of biotin-HPDP on gold surface. The broad peak at 1674 cm^{-1} was due to the amide-1 bands of biotin-HPDP, peak at 2942 cm^{-1} was due to the CH_2 stretching vibrations of alkyl chains and peak at 3328 cm^{-1} was due to the secondary amide N-H stretching. The peak at 538 cm^{-1} was due to the presence of disulphide bond of biotin-HPDP which was not observed after its reduction with butylphosphine. The thiol-capped biotin immobilized on gold was able to capture the streptavidin-conjugated nanoparticles as demonstrated by SEM images that show particles that remain after washing. The size of the functionalized particles was not uniform due to some aggregation nature. EDS analysis confirmed the presence of nanoparticles on the biotinylated gold surface as well. The intensity of EDS signal was directly proportional to the size of the particle that is confirmed by the increase in the

intensity of iron signal as the particle's size increases. But there was a high carbon signal compared to iron observed from the small particles. The possible reason for this might be heavily aggregated particles may have less streptavidin bonded to them. FT-IR spectra and fluorescent images also confirmed the nanoparticle capture on botinylated gold surface, albeit with less resolution. Aminated glass surfaces were used for the immobilization of sulpho NHS-biotin. Following biotinylation these glass surfaces were functionalized with streptavidin-FITC nanoparticles. Fluorescent images confirmed the specific binding of nanoparticles to the functionalized aminated surface. SEM confirmed the aggregation nature of particles and average size of the particles found was $106.58 \pm 46.36 \text{ nm}$ which are less compared to the previous works which used purchased nanoparticles with size in the range of 200nm. Also aminated glass substrates were helpful in eliminating the background problems associated with gold when imaging the functionalization of nanoparticles with fluorescent microscopy.

This study is different from a similar work using magnetic particles, spacers, and surfactants for detection systems (Arakaki 2004). Arakaki's group used Octadecyltrimethoxysilane (ODMS) as a spacer to avoid nonspecific adsorption of nanoparticles whereas in our technique an internal spacer to the biotin-HPDP, pyridine 2-thiol, was used to functionalize the gold surfaces and no spacer was used to functionalize glass surfaces with sulpho-NHS biotin. Sodium dodecylsulphate (SDS) was used as a surfactant to minimize the aggregation of particles whereas in our study no surfactant was used. Additionally, 3-aminopropyltriethoxysilane (APS) was used as a linker between the surface and sulpho-NHS-LC-LC-biotin whereas in our study the self assembled monolayers of biotin-HPDP and sulpho NHS biotin were formed on gold or

aminated glass substrates directly. The amine groups of purchased magnetite nanoparticles were reacted with sulpho-NHS-LC-LC-biotin and then functionalized with streptavidin whereas in our study direct functionalization of synthesized nanoparticles with streptavidin was done by using EDC chemistry. Linked layers of nanoparticle-biotin-streptavidin-biotin-SAM were characterized by optical microscopy, magnetic force microscopy (MFM), and scanning electron microscopy (SEM) whereas in our study Fourier transform infrared spectroscopy (FT-IR), fluorescent microscopy, scanning electron microscopy (SEM), Transmission electron microscopy (TEM), and X-ray photoelectron microscopy (XPS) were used to characterize the surfaces.

In summary, these techniques have application in studying the modification and behavior of nanoparticles for biological and other applications such as measuring low concentrations of bacteria, more efficient site-specific drug delivery, detection of proteins, and separation and purification of biological molecules and cells. The detection of low concentrations of bacteria is an important consideration in developing new and robust biosensors. By using principles of DNA hybridization, functionalized magnetic nanoparticles, and GMR, it is possible to measure the low concentrations of bacteria similar to that seen in the BARC sensor. The results of this study have shown that nanoparticles can be functionalized and they can be immobilized onto a biotinylated gold substrate using bimolecular interactions.

3.2 Future Considerations

When small nanoparticles are dispersed in microfluid, the permanent magnetization is evenly distributed throughout the fluid and hence gets compensated. This prevents particles from agglomeration. As the particle size increases, the magnetic

interactions between particles predominate leading to particle agglomeration. A further study to decrease the degree of aggregation is a worthwhile endeavor. One possible solution might be use of surfactant such as oleic acid to coat the nanoparticle surface during synthesis to prevent them from aggregation (Horak 2003). Sodium dodecyl sulphate (SDS) could also be used at each step in the synthesis and functionalization of nanoparticles. Additionally, the use of freshly-prepared nanoparticles is a better practice to avoid aggregation because of the likelihood to aggregate over longer periods alone in solution. The effect of SDS on binding capacity of nanoparticles and on fluorescence of nanoparticles will be useful to know the use of SDS to prevent aggregation of nanoparticles. Zirconia nanoparticles could also potentially be used as a surfactant to avoid the aggregation, especially when they are used to bind to biotinylated gold surfaces (Han 2004).

Because non-specific binding is problematic while functionalizing surfaces, a study comparing the effect of PEG and pyridine 2-thiol as a spacer would be interesting, as relatively little work has been done in this area.

In this study, FITC-labeled streptavidin has been used to functionalize nanoparticles. Different kinds of fluorophores such as Texas red, DAPI, and others can be used to functionalize the nanoparticles for multicolor analysis of multiparameter detection. By comparing the fluorescence from newer more stable dyes, photo-bleaching effects can also be determined, although this was not seen in our study to a significant degree.

In this study, characterization of particles is done using TEM and SEM. A better technique is needed to characterize the immobilized nanoparticles on the gold

substrates to image nanoparticles. Atomic Force Microscopy (AFM) is an alternative technique to get better resolution at nanometer scales. Magnetic force microscopy (MFM) can also be used to confirm the spatial arrangement of magnetic nanoparticles (Arakaki 2004).

Employment of GMR sensors for the detection of functionalized nanoparticles is of increasing interest to the field of biosensing. Immobilization of oligonucleotides onto the GMR and hybridization with complementary biotinylated DNA, followed by detection of functionalized nanoparticles may have greater benefit in the detection of low concentrations of bacteria compared to microparticle techniques. The magnetization per unit weight of nanoparticles is higher than that of micro-particles, and the number of particles present in 1 mg of solution can have 10^8 times more nanoparticles than micro-particles. These facts indicate that number of particles that can bind to streptavidin is greater, and that the sensitivity of magnetic nanoparticle based biosensor is higher. Here we have identified several possible means to functionalize and characterize these interactions that will hopefully lead to more sensitive and rapid detection.

References

- Ago, H., T. Komatsu, S. Ohshima, Y. Kuriki and M. Yumura (2000). "Dispersion of metal nanoparticles for aligned carbon nanotube arrays." *Applied Physics Letters* 77(1): 79-81.
- Arakaki, A., S. Hideshima, T. Nakagawa, D. Niwa, T. Tanaka, T. Matsunaga and T. Osaka (2004). "Detection of biomolecular interaction between biotin and streptavidin on a self-assembled monolayer using magnetic nanoparticles." *Biotechnology and Bioengineering* 88(4): 543-546.
- Artemov, D., N. Mori, B. Okollie and Z. M. Bhujwala (2003). "MR molecular imaging of the Her-2/neu receptor in breast cancer cells using targeted iron oxide nanoparticles." *Magnetic Resonance in Medicine* 49(3): 403-408.
- Aslam, M., K. Bandyopadhyay, K. Vijayamohan and V. Lakshminarayanan (2001). "Comparative behavior of aromatic disulfide and diselenide monolayers on polycrystalline gold films using cyclic voltammetry, STM, and quartz crystal microbalance." *Journal of Colloid and Interface Science* 234(2): 410-417.
- Aslan, K., J. R. Lakowicz and C. D. Geddes (2004). "Nanogold-plasmon-resonance-based glucose sensing." *Analytical Biochemistry* 330(1): 145-155.
- Balzer, F., R. Gerlach, G. Polanski and H. G. Rubahn (1997). "Chain length dependence of the structure of alkane thiol films on Au(111)." *Chemical Physics Letters* 274(1-3): 145-151.
- Bandyopadhyay, K., M. Sastry, V. Paul and K. Vijayamohan (1997). "Formation of a redox active self-assembled monolayer: Naphtho[1,8-cd]-1,2-dithiol on gold." *Langmuir* 13(4): 866-869.
- Beiser, A. (1973). *Modern technical physics*. Menlo park, cummings publishing company.
- Besse, P. A., G. Boero, M. Demierre, V. Pott and R. Popovic (2002). "Detection of a single magnetic microbead using a miniaturized silicon Hall sensor." *Applied Physics Letters* 80(22): 4199-4201.
- Blum, E. C. A., Maiorov M.M (1997). *Magnetic Fluids*. Berlin, Walter de Gruyter.
- Boncheva, M., D. A. Bruzewicz and G. M. Whitesides (2003). "Millimeter-scale self-assembly and its applications." *Pure and Applied Chemistry* 75(5): 621-630.
- Brannon-Peppas, L. (2000). "Poly(ethylene glycol): Chemistry and Biological Applications - J.M. Harris and S. Zalipsky, editors, American Chemical Society, Washington DC, 1997, 489 pp." *Journal of Controlled Release* 66: 321.

- Bucak, S., D. A. Jones, P. E. Laibinis and T. A. Hatton (2003). "Protein separations using colloidal magnetic nanoparticles." *Biotechnology Progress* 19(2): 477-484.
- Callow, M. E., J. A. Callow, L. K. Ista, S. E. Coleman, A. C. Nolasco and G. P. Lopez (2000). "Use of self-assembled monolayers of different wettabilities to study surface selection and primary adhesion processes of green algal (*Enteromorpha*) zoospores." *Appl Environ Microbiol* 66(8): 3249-54.
- Cao, J. Q., Y. X. Wang, J. F. Yu, J. Y. Xia, C. F. Zhang, D. Z. Yin and U. O. Hafeli (2004). "Preparation and radiolabeling of surface-modified magnetic nanoparticles with rhenium-188 for magnetic targeted radiotherapy." *Journal of Magnetism and Magnetic Materials* 277(1-2): 165-174.
- Cao, Y. C., R. Jin, J. M. Nam, C. S. Thaxton and C. A. Mirkin (2003). "Raman dye-labeled nanoparticle probes for proteins." *J Am Chem Soc* 125(48): 14676-7.
- Chan, D. C. F., D. B. Kirpotin and P. A. Bunn (1993). "Synthesis and Evaluation of Colloidal Magnetic Iron-Oxides for the Site-Specific Radiofrequency-Induced Hyperthermia of Cancer." *Journal of Magnetism and Magnetic Materials* 122(1-3): 374-378.
- Chang, Y. C. and D. H. Chen (2005). "Preparation and adsorption properties of monodisperse chitosan-bound Fe₃O₄ magnetic nanoparticles for removal of Cu(II) ions." *Journal of Colloid and Interface Science* 283(2): 446-451.
- Chapman, R. G., E. Ostuni, M. N. Liang, G. Meluleni, E. Kim, L. Yan, G. Pier, H. S. Warren and G. M. Whitesides (2001). "Polymeric thin films that resist the adsorption of proteins and the adhesion of bacteria." *Langmuir* 17(4): 1225-1233.
- Chemla, Y. R., H. L. Crossman, Y. Poon, R. McDermott, R. Stevens, M. D. Alper and J. Clarke (2000). "Ultrasensitive magnetic biosensor for homogeneous immunoassay." *Proceedings of the National Academy of Sciences of the United States of America* 97(26): 14268-14272.
- Chen, D. H. and M. H. Liao (2002). "Preparation and characterization of YADH-bound magnetic nanoparticles." *Journal of Molecular Catalysis B-Enzymatic* 16(5-6): 283-291.
- Chidsey, C. E. D. and D. N. Loiacono (1990). "Chemical Functionality in Self-Assembled Monolayers - Structural and Electrochemical Properties." *Langmuir* 6(3): 682-691.
- Cornell, R. M., S. U. (1996). *The Iron Oxides: Structure, Properties, Reactions, Occurrence and Uses*. Weinheim, VCH Publishers.
- Cornell, R. M., S. U. (1991). *Iron Oxides in the Laboratory; Preparation and Characterization*. Weinheim, VCH.

curtis.A, A. K. G. a. (2002). "Surface modification of superparamagnetic ironoxide nanoparticles and their intracellular uptake." *European cells and materials* 4(2): 101-102.

Delamarche, E., B. Michel, H. A. Biebuyck and C. Gerber (1996). "Golden interfaces: The surface of self-assembled monolayers." *Advanced Materials* 8(9): 719-8.

Dubois, L. H. and R. G. Nuzzo (1992). "Synthesis, Structure, and Properties of Model Organic-Surfaces." *Annual Review of Physical Chemistry* 43: 437-463.

Edelstein, R. L., C. R. Tamana, P. E. Sheehan, M. M. Miller, D. R. Baselt, L. J. Whitman and R. J. Colton (2000). "The BARC biosensor applied to the detection of biological warfare agents." *Biosensors & Bioelectronics* 14(10-11): 805-813.

Edinger, K., A. Golzhauser, K. Demota, C. Woll and M. Grunze (1993). "Formation of Self-Assembled Monolayers of N-Alkanethiols on Gold - a Scanning Tunneling Microscopy Study on the Modification of Substrate Morphology." *Langmuir* 9(1): 4-8.

Elbert, D. L. and J. A. Hubbell (1996). "Surface treatments of polymers for biocompatibility." *Annual Review of Materials Science* 26: 365-394.

Forbes, Z. G., B. B. Yellen, K. A. Barbee and G. Friedman (2003). "An approach to targeted drug delivery based on uniform magnetic fields." *IEEE Transactions on Magnetism* 39(5): 3372-3377.

Fritzsche, W., E. Ermantraut and J. M. Kohler (1998). "Characterization of biomolecule immobilization by scanning force microscopy using a wet-masking technique." *Scanning* 20(2): 106-109.

Gan, X., T. Liu, X. L. Zhu and G. X. Li (2004). "An electrochemical biosensor for nitric oxide based on silver nanoparticles and hemoglobin." *Analytical Sciences* 20(9): 1271-1275.

Gau, J. J., E. H. Lan, B. Dunn, C. M. Ho and J. C. S. Woo (2001). "A MEMS based amperometric detector for E-Coli bacteria using self-assembled monolayers." *Biosensors & Bioelectronics* 16(9-12): 745-755.

Gilchrist, R. K., R. Medal, W. D. Shorey, R. C. Hanselman, J. C. Parrott and C. B. Taylor (1957). "Selective inductive heating of lymph nodes." *Ann Surg* 146(4): 596-606.

Giorgi, R., L. Dei, M. Ceccato, C. Schettino and P. Baglioni (2002). "Nanotechnologies for conservation of cultural heritage: Paper and canvas deacidification." *Langmuir* 18(21): 8198-8203.

Gupta, A. K. and S. Wells (2004). "Surface-modified superparamagnetic nanoparticles for drug delivery: Preparation, characterization, and cytotoxicity studies." *IEEE Transactions on Nanobioscience* 3(1): 66-73.

Han, S. J., T. K. Yu, J. Park, B. Koo, J. Joo, T. Hyeon, S. Hong and J. Im (2004). "Diameter-controlled synthesis of discrete and uniform-sized single-walled carbon nanotubes using monodisperse iron oxide nanoparticles embedded in zirconia nanoparticle arrays as catalysts." *Journal of Physical Chemistry B* 108(24): 8091-8095.

Heuberger, M., T. Drobek and N. D. Spencer (2005). "Interaction forces and morphology of a protein-resistant poly(ethylene glycol) layer." *Biophysical Journal* 88(1): 495-504.

Hiergeist, R., W. Andra, N. Buske, R. Hergt, I. Hilger, U. Richter and W. Kaiser (1999). "Application of magnetite ferrofluids for hyperthermia." *Journal of Magnetism and Magnetic Materials* 201: 420-422.

Hilger, I., A. Kiessling, E. Romanus, R. Hiergeist, H. T. Rudolf, W. Andra, M. Roskos, W. Linss, P. Weber, W. Weitschies and W. A. Kaiser (2004). "Magnetic nanoparticles for selective heating of magnetically labelled cells in culture: preliminary investigation." *Nanotechnology* 15(8): 1027-1032.

Horak, D., N. Semenyuk and F. Lednicky (2003). "Effect of the reaction parameters on the particle size in the dispersion polymerization of 2-hydroxyethyl and glycidyl methacrylate in the presence of a ferrofluid." *Journal of Polymer Science Part a-Polymer Chemistry* 41(12): 1848-1863.

Hou, T., M. Greenlief, S. W. Keller, L. Nelen and J. F. Kauffman (1997). "Passivation of GaAs (100) with an adhesion promoting self-assembled monolayer." *Chemistry of Materials* 9(12): 3181-3186.

Huhtinen, P., T. Soukka, T. Lovgren and H. Harma (2004). "Immunoassay of total prostate-specific antigen using europium(III) nanoparticle labels and streptavidin-biotin technology." *Journal of Immunological Methods* 294(1-2): 111-122.

Jennings, G. K., J. C. Munro, T. H. Yong and P. E. Laibinis (1998). "Effect of chain length on the protection of copper by n-alkanethiols." *Langmuir* 14(21): 6130-6139.

Jeon, S. I., J. H. Lee, J. D. Andrade and P. G. Degennes (1991). "Protein Surface Interactions in the Presence of Polyethylene Oxide.1. Simplified Theory." *Journal of Colloid and Interface Science* 142(1): 149-158.

Katz, E., R. Baron and I. Willner (2005). "Magnetoswitchable electrochemistry gated by alkyl-chain-functionalized magnetic nanoparticles: Control of diffusional and surface-confined electrochemical processes." *Journal of the American Chemical Society* 127(11): 4060-4070.

Kittel, C. (1946). "Theory of the Structure of Ferromagnetic Domains in Films and Small Particles." *Physical Reviews* 70(11-12): 965–971.

Kittel, C. (1976). "Introduction to solid state physics."

Kumar, C. S., C. Leuschner, E. E. Doomes, L. Henry, M. Juban and J. Hormes (2004). "Efficacy of lytic peptide-bound magnetite nanoparticles in destroying breast cancer cells." *J Nanosci Nanotechnol* 4(3): 245-9.

LesliePelecky, D. L. and R. D. Rieke (1996). "Magnetic properties of nanostructured materials." *Chemistry of Materials* 8(8): 1770-1783.

Li, G. Y., H. Y. Ma, Y. L. Jiao and S. H. Chen (2004). "An impedance investigation of corrosion protection of copper by self-assembled monolayers of alkanethiols in aqueous solution." *Journal of the Serbian Chemical Society* 69(10): 791-805.

Li, H., E. Burts, K. Bears, Q. Ji, J. J. Lesko, D. A. Dillard, J. S. Riffle and P. M. Puckett (2000). "Network structure and properties of dimethacrylate-styrene matrix materials." *Journal of Composite Materials* 34(18): 1512-1528.

Li, H., A. C. Rosario, S. V. Davis, T. Glass, T. V. Holland, R. M. Davis, J. J. Lesko, J. S. Riffle and J. Florio (1997). "Network formation of vinylester-styrene composite matrix resins." *Journal of Advanced Materials* 28(4): 55-62.

Li, Y. Q., P. Xiong, S. von Molnar, S. Wirth, Y. Ohno and H. Ohno (2002). "Hall magnetometry on a single iron nanoparticle." *Applied Physics Letters* 80(24): 4644-4646.

Lu, H. C., G. S. Yi, S. Y. Zhao, D. P. Chen, L. H. Guo and J. Cheng (2004). "Synthesis and characterization of multi-functional nanoparticles possessing magnetic, up-conversion fluorescence and bio-affinity properties." *Journal of Materials Chemistry* 14(8): 1336-1341.

Lubbe, A. S., C. Alexiou and C. Bergemann (2001). "Clinical applications of magnetic drug targeting." *Journal of Surgical Research* 95(2): 200-206.

Margaret V. Merritt, M. M., George M. Whitesides (1997). *Using Self-Assembled Monolayers to Study the Interactions of Man-Made Materials with Proteins*. Georgetown TX, Principles of Tissue Engineering, R.G. Landes Company.

Maxwell, D. J., J. R. Taylor and S. M. Nie (2002). "Self-assembled nanoparticle probes for recognition and detection of biomolecules." *Journal of the American Chemical Society* 124(32): 9606-9612.

Mirsky, V. M., M. Vasjari, I. Novotny, V. Rehacek, V. Tvarozek and O. S. Wolfbeis (2002). "Self-assembled monolayers as selective filters for chemical sensors." *Nanotechnology* 13(2): 175-178.

Molday, R. S. and D. Mackenzie (1982). "Immunospecific Ferromagnetic Iron-Dextran Reagents for the Labeling and Magnetic Separation of Cells." *Journal of Immunological Methods* 52(3): 353-367.

Moller, W., I. Nemoto and J. Heyder (2003). "Effect of magnetic bead agglomeration on cytomagnetometric measurements." *IEEE Transactions on Nanobioscience* 2(4): 247-254.

Morales, M. P., M. Andres-Verges, S. Veintemillas-Verdaguer, M. I. Montero and C. J. Serna (1999). "Structural effects on the magnetic properties of gamma-Fe₂O₃ nanoparticles." *Journal of Magnetism and Magnetic Materials* 203: 146-148.

Mourougou-Candoni, N., C. Naud and F. Thibaudau (2003). "Adsorption of thiolated oligonucleotides on gold surfaces: An atomic force microscopy study." *Langmuir* 19(3): 682-686.

Mrksich, M., G. B. Sigal and G. M. Whitesides (1995). "Surface-Plasmon Resonance Permits in-Situ Measurement of Protein Adsorption on Self-Assembled Monolayers of Alkanethiolates on Gold." *Langmuir* 11(11): 4383-4385.

Ozaki, M. (2000). *Fine Particles: Synthesis, Characterization, and Mechanisms of Growth*. New York, Marcel Dekker, Inc.

Pan, B. F., F. Gao and H. C. Gu (2005). "Dendrimer modified magnetite nanoparticles for protein immobilization." *Journal of Colloid and Interface Science* 284(1): 1-6.

Pan, J., N. Tao and S. M. Lindsay (1993). "An Atomic-Force Microscopy Study of a Self-Assembled Octadecyl Mercaptan Monolayer Adsorbed on Gold(111) under Potential Control." *Langmuir* 9(6): 1556-1560.

Pankhurst, Q. A., J. Connolly, S. K. Jones and J. Dobson (2003). "Applications of magnetic nanoparticles in biomedicine." *Journal of Physics D-Applied Physics* 36(13): R167-R181.

Peng, H. B., T. G. Ristorph, G. M. Schurmann, G. M. King, J. Yoon, V. Narayanamurti and J. A. Golovchenko (2003). "Patterned growth of single-walled carbon nanotube arrays from a vapor-deposited Fe catalyst." *Applied Physics Letters* 83(20): 4238-4240.

Perez, J. M., T. O'Loughin, F. J. Simeone, R. Weissleder and L. Josephson (2002). "DNA-based magnetic nanoparticle assembly acts as a magnetic relaxation nanoswitch allowing screening of DNA-cleaving agents." *Journal of the American Chemical Society* 124(12): 2856-2857.

Popplewell, J. and L. Sakhnini (1995). "The Dependence of the Physical and Magnetic-Properties of Magnetic Fluids on Particle-Size." *Journal of Magnetism and Magnetic Materials* 149(1-2): 72-78.

Pradier, C. M., M. Salmain, Z. Liu and C. Methivier (2002). "Comparison of different procedures of biotin immobilization on gold for the molecular recognition of avidin: an FT-IRRAS study." *Surface and Interface Analysis* 34(1): 67-71.

Pradier, C. M., M. Salmain, L. Zheng and G. Jaouen (2002). "Specific binding of avidin to biotin immobilised on modified gold surfaces - Fourier transform infrared reflection absorption spectroscopy analysis." *Surface Science* 502: 193-202.

Prime, K. L. and G. M. Whitesides (1993). "Adsorption of Proteins onto Surfaces Containing End-Attached Oligo(Ethylene Oxide) - a Model System Using Self-Assembled Monolayers." *Journal of the American Chemical Society* 115(23): 10714-10721.

Riepl, M., K. Enander, B. Liedberg, M. Schaferling, M. Kruschina and F. Ortigao (2002). "Functionalized surfaces of mixed alkanethiols on gold as a platform for oligonucleotide microarrays." *Langmuir* 18(18): 7016-7023.

Rife, J. C., M. M. Miller, P. E. Sheehan, C. R. Tamanaha, M. Tondra and L. J. Whitman (2003). "Design and performance of GMR sensors for the detection of magnetic microbeads in biosensors." *Sensors and Actuators a-Physical* 107(3): 209-218.

Rosensweig, R. E. (2002). "Heating magnetic fluid with alternating magnetic field." *Journal of Magnetism and Magnetic Materials* 252(1-3): 370-374.

Rossi, L. M., A. D. Quach and Z. Rosenzweig (2004). "Glucose oxidase-magnetite nanoparticle bioconjugate for glucose sensing." *Analytical and Bioanalytical Chemistry* 380(4): 606-613.

Sahoo, Y., A. Goodarzi, M. T. Swihart, T. Y. Ohulchanskyy, N. Kaur, E. P. Furlani and P. N. Prasad (2005). "Aqueous ferrofluid of magnetite nanoparticles: Fluorescence labeling and magnetophoretic control." *Journal of Physical Chemistry B* 109(9): 3879-3885.

Sato, T., T. Iijima, M. Seki and N. Inagaki (1987). "Magnetic-Properties of Ultrafine Ferrite Particles." *Journal of Magnetism and Magnetic Materials* 65(2-3): 252-256.

Shumaker-Parry, J. S., M. H. Zareie, R. Aebersold and C. T. Campbell (2004). "Microspotting streptavidin and double-stranded DNA Arrays on gold for high-throughput studies of protein-DNA interactions by surface plasmon resonance microscopy." *Analytical Chemistry* 76(4): 918-929.

- Smit, J. W. H. P. J. (1959). Ferrites. New York, John Wiley & Sons.
- Sorensen, C. M. (2001). Nanoscale Materials in Chemistry. New York, John Wiley and Sons Inc.
- Spinke, J., M. Liley, F. J. Schmitt, H. J. Guder, L. Angermaier and W. Knoll (1993). "Molecular Recognition at Self-Assembled Monolayers - Optimization of Surface Functionalization." *Journal of Chemical Physics* 99(9): 7012-7019.
- Sqalli, O., M. P. Bernal, P. Hoffmann and F. Marquis-Weible (2000). "Improved tip performance for scanning near-field optical microscopy by the attachment of a single gold nanoparticle." *Applied Physics Letters* 76(15): 2134-2136.
- Sun, L. and R. M. Crooks (1993). "Indirect Visualization of Defect Structures Contained within Self-Assembled Organomercaptan Monolayers - Combined Use of Electrochemistry and Scanning-Tunneling-Microscopy." *Langmuir* 9(8): 1951-1954.
- Sun, S. H., S. Anders, H. F. Hamann, J. U. Thiele, J. E. E. Baglin, T. Thomson, E. E. Fullerton, C. B. Murray and B. D. Terris (2002). "Polymer mediated self-assembly of magnetic nanoparticles." *Journal of the American Chemical Society* 124(12): 2884-2885.
- Takahashi, S. and S. Maekawa (1998). "Effect of Coulomb blockade on magnetoresistance in ferromagnetic tunnel junctions." *Physical Review Letters* 80(8): 1758-1761.
- Tartaj, P., M. D. Morales, S. Veintemillas-Verdaguer, T. Gonzalez-Carreno and C. J. Serna (2003). "The preparation of magnetic nanoparticles for applications in biomedicine." *Journal of Physics D-Applied Physics* 36(13): R182-R197.
- Tebble R. S, C. D. J. (1969). *Magnetic Materials*. London, Wiley-Interscience.
- Tebble R. S, C. D. J. (1996). *Magnetic Materials*, Wiley-Interscience.
- Teng, X. W. and H. Yang (2004). "Effects of surfactants and synthetic conditions on the sizes and self-assembly of monodisperse iron oxide nanoparticles." *Journal of Materials Chemistry* 14(4): 774-779.
- Tien, J., A. Terfort and G. M. Whitesides (1997). "Microfabrication through electrostatic self-assembly." *Langmuir* 13(20): 5349-5355.
- Tosatti, S. (2003). "Functionalized Titanium Surfaces for Biomedical Applications: Physico-chemical Characterization and Biological in vitro Evaluation." Department of Materials, ETH: Zürich.

Trenary, M. (2000). "Reflection absorption infrared spectroscopy and the structure of molecular adsorbates on metal surfaces." *Annual Review of Physical Chemistry* 51: 381-403.

Turgut Aytur, P. R. B., Bernhard Boser, Mekhail Anwar, Tomohiro Ishikawa (2002). "An Immunoassay Platform Based on CMOS Hall Sensors." *Solid-State Sensor, Actuator and Microsystems Workshop*: 126-129.

Ulman, A. (1996). "Formation and structure of self-assembled monolayers." *Chemical Reviews* 96(4): 1533-1554.

Venkataramanan, M., G. Skanth, K. Bandyopadhyay, K. Vijayamohanan and T. Pradeep (1999). "Self-assembled monolayers of two aromatic disulfides and a diselenide on polycrystalline silver films: An investigation by SERS and XPS." *Journal of Colloid and Interface Science* 212(2): 553-561.

Voldman, J., M. L. Gray and M. A. Schmidt (1999). "Microfabrication in biology and medicine." *Annual Review of Biomedical Engineering* 1: 401-425.

Walczak, M. M., D. D. Popenoe, R. S. Deinhammer, B. D. Lamp, C. K. Chung and M. D. Porter (1991). "Reductive Desorption of Alkanethiolate Monolayers at Gold - a Measure of Surface Coverage." *Langmuir* 7(11): 2687-2693.

Waldron, R. D. (1955). "Infrared Spectra of ferrites." *Physical review* 99(6): 1727-1735.

Weller, D. and A. Moser (1999). "Thermal effect limits in ultrahigh-density magnetic recording." *IEEE Transactions on Magnetics* 35(6): 4423-4439.

Whelan, C. M., M. Kinsella, H. M. Ho and K. Maex (2004). "In-situ cleaning and passivation of oxidized Cu surfaces by alkanethiols and its application to wire bonding." *Journal of Electronic Materials* 33(9): 1005-1011.

Whitesides, G. M. and P. E. Laibinis (1990). "Wet Chemical Approaches to the Characterization of Organic-Surfaces - Self-Assembled Monolayers, Wetting, and the Physical Organic-Chemistry of the Solid Liquid Interface." *Langmuir* 6(1): 87-96.

Wink, T., S. J. vanZuilen, A. Bult and W. P. vanBennekom (1997). "Self-assembled monolayers for biosensors." *Analyst* 122(4): R43-R50.

Xu, J. J., W. Zhao, X. L. Luo and H. Y. Chen (2005). "A sensitive biosensor for lactate based on layer-by-layer assembling MnO₂ nanoparticles and lactate oxidase on ion-sensitive field-effect transistors." *Chemical Communications*(6): 792-794.

Yam, C. M., C. M. Pradier, M. Salmain, N. Fischer-Durand and G. Jaouen (2002). "Molecular recognition of avidin on biotin-functionalized gold surfaces detected by FT-

IRRAS and use of metal carbonyl probes." *Journal of Colloid and Interface Science* 245(1): 204-207.

Yan, M. D., S. X. Cai, M. N. Wybourne and J. F. W. Keana (1993). "Photochemical Functionalization of Polymer Surfaces and the Production of Biomolecule-Carrying Micrometer-Scale Structures by Deep-Uv Lithography Using 4-Substituted Perfluorophenyl Azides." *Journal of the American Chemical Society* 115(2): 814-816.

Yan, M. D., S. X. Cai, M. N. Wybourne and J. F. W. Keana (1994). "N-Hydroxysuccinimide Ester Functionalized Perfluorophenyl Azides as Novel Photoactive Heterobifunctional Cross-Linking Reagents - the Covalent Immobilization of Biomolecules to Polymer Surfaces." *Bioconjugate Chemistry* 5(2): 151-157.

Yang, H. H., S. Q. Zhang, X. L. Chen, Z. X. Zhuang, J. G. Xu and X. R. Wang (2004). "Magnetite-containing spherical silica nanoparticles for biocatalysis and bioseparations." *Analytical Chemistry* 76(5): 1316-1321.

Zhang, F., E. T. Kang, K. G. Neoh and W. Huang (2001). "Modification of gold surface by grafting of poly(ethylene glycol) for reduction in protein adsorption and platelet adhesion." *Journal of Biomaterials Science-Polymer Edition* 12(5): 515-531.

Zhang, Y. and J. Zhang (2005). "Surface modification of monodisperse magnetite nanoparticles for improved intracellular uptake to breast cancer cells." *Journal of Colloid and Interface Science* 283(2): 352-357.

Zimmermann, R. M. and E. C. Cox (1994). "DNA stretching on functionalized gold surfaces." *Nucleic Acids Res* 22(3): 492-7.

Vita

Giri Nidumolu was born on the 6th of June, 1979, in Machilipatnam, Andhra Pradesh, to Narayana Rao Nidumolu and Syamala Nidumolu. He attended high school at A.J.K Oriental Secondary School, where he graduated with honors in 1994. He attended intermediate school at A. J. Kalasala, where he graduated with honors in 1996. Following high school, Giri enrolled at Jawaharlal Nehru Technological University in Hyderabad, Andhra Pradesh, where he graduated with honors with a Bachelor of Technology in Electrical and Electronics Engineering. Upon completion of his degree, he spent one semester of graduate study at the University of South Florida studying for a master of science in electrical engineering. He joined Louisiana State University in the fall of 2002 and is currently enrolled as a candidate for the degree of Master of Science in Biological and Agricultural Engineering, which will be awarded in May 2005.